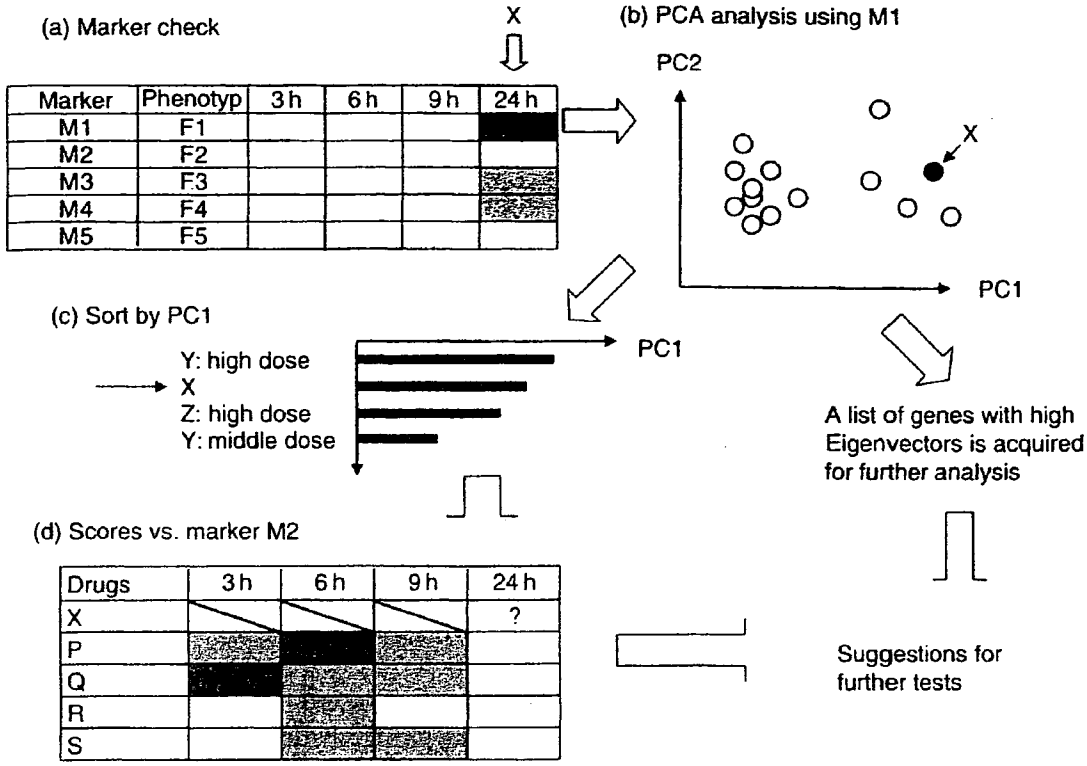

Figure 20.9 *Schematic representation of an image of toxicity prediction process in the TGP system. (a) The data of new drug X that are up-loaded to the TGP system are checked against several markers useful to predict phenotypes in repeated administration from single-dose experiments. One of the markers (M1) shows an alert. (b) PCA is performed using these marker genes, M1. X is clearly separated in the direction of PC1 with high contribution value. Then, the compounds are sorted by PC1, showing the order of Y (high dose) > X > Z (high dose) > Y (middle dose). The gene list with high Eigenvectors can be harvested for further analysis. (c) Drugs P and Q cause phenotype F2. The marker M2, predicting future phenotype F2, is available in the database. When compounds, including X, are overviewed against M2, not only X but also P and Q show low scores at 24 h while the latter two show high scores in this marker gene list at earlier periods. This indicates that prediction of F2 is inconclusive without the expression data in earlier stages*

of candidate drugs are usually done just before the clinical trial. If serious toxicity emerges at this stage, it might be necessary to return to the seeds, because toxicity is often inherent to the basic structure and thus never eliminated by minor modification. If the potential phenotype (when repeatedly dosed) is predictable in the early stage by gene expression data of a few numbers of experimental animals, it would effectively cut out time and cost for drug development. From another point of view, this also contributes to animal welfare by reducing the number of sacrifices.

Application of toxicogenomics to the toxicity test in the final candidate just before clinical trials seems to be promising to improve the predictivity of clinical side effects. In fact there is a trend to employ toxicogenomics and pharmacogenomics technology for regulatory science (Petit, 2004). In such a case, various issues regarding validation and

standardization of data acquisition and analysis in addition to the species difference will be problems that should be solved urgently.

The third field for toxicogenomics is post-marketing surveillance. One promising strategy against species difference would be the connection of the clinical data to the TGP database. As human *in vivo* experiments are impossible and the barrier between *in vivo* and *in vitro* is too high, the only way is to accumulate clinical phenomena that are related to the contents in the database. There is a movement to create databases of disease-related genotypes or SNPs, and it would be promising to make a functional network between these databases and the TGP to establish an integrated toxico/pharmacogenomics database.

In any event, the completion of the TGP database is not a goal, but a beginning for toxicogenomics study. Compared with the enrichment of the data, the analysis/prediction procedures are in the developing stage. It is our desire that toxicology together with systems biology rapidly advances by efficient use of this database and that it contributes in accelerating the development of more effective and safer drugs.

Acknowledgments

The following researchers were involved in the project until this paper was written. Taku Nagao (Project Leader), Toshikazu Miyagishima (Sub-Leader), Ken-ichi Aisaki, Takanobu Hanada, Satoru Hashimoto, Masayuki Heishi, Mituhiro Hirode, Akihiko Hirose, Takehiko Hosoiri, Katsuhide Igarashi, Shoichiro Ide, Dai Kakiuchi, Jun Kanno, Toshihiko Kasahara, Naoki Kiyosawa, Masanobu Komiya, Tomochika Matushita, Toshiko Miyazaki, Yumiko Mizukawa, Katsumi Morishita, Takamichi Muramatsu, Hiroyuki Nitta, Yoshie Ohno, Manabu Okuyama, Ko Omura, Atsushi Ono, Yoshiyuki Saeki, Atsushi Shibutani, Toshinori Shimizu, Tunefumi Shiwaku, Takamasa Suzuki, Kayoko Takashima, Kotaro Tamura, Hiroyuki Tomita, Naoki Torizuka, Hirohiko Totsuka, Soh Tsunezuka, Hiroyuki Ueda, Takeki Uehara and Tomoya Yamashita.

Half of the project was supported by a grant from the Ministry of Health, Labour and Welfare, H14-toxico-001.

References

Boess, F., Kamber, M., Romer, S., Gasser, R., Muller, D., Albertini, S. and Suter, L. (2003). Gene expression in two hepatic cell lines, cultured primary hepatocytes, and liver slices compared to the *in vivo* liver gene expression in rats: possible implications for toxicogenomics use of *in vitro* systems. *Toxicol Sci* **73**, 386–402.

Boverhof, D. R. and Zacharewski, T. R. (2006). Toxicogenomics in risk assessment: applications and needs. *Toxicol Sci* **89**, 352–360.

Brown, M. P., Grundy, W. N., Lin, D., Cristianini, N., Sugnet, C. W., Furey, T. S., Ares, M. Jr and Haussler, D. (2000). Knowledge-based analysis of microarray gene expression data by using support vector machines. *Proc Natl Acad Sci USA* **97**, 262–267.

Draghici, S. (2003). Analysis and visualization tools, in *Data Analysis Tools for DNA Microarrays*; A. M. Etheridge, L. J. Gross, S. Lenhart, P. K. Maini, H. M. Safer and E. O. Voit (Eds), CRC Press, London, UK, pp. 231–261.

Ismail, K. and Landis, J. (2003). Can the pharmaceutical industry reduce attrition rates? *Nat Rev Drug Discov* **3**, 711–715.

James, L. P., Mayeux, P. R. and Hinson, J. A. (2003). Acetaminophen-induced hepatotoxicity. *Drug Metab Dispos* **31**, 1499–1506.

Kaminski, N. and Friedman, N. (2002). Practical approaches to analyzing results of microarray experiments. *Am J Respir Cell Mol Biol* **27**, 125–132.

Kanno, J., Aisaki, K., Igarashi, K., Nakatsu, N., Ono, A., Kodama, Y. and Nagao, T. (2006). 'Per cell' normalization method for mRNA measurement by quantitative PCR and microarrays. *BMC Genom*, **7**, 64.

Kiyosawa, N., Ito, K., Sakuma, K., Niino, N., Kanbori, M., Yamoto, T., Manabe, S. and Matsunuma, N. (2004). Evaluation of glutathione deficiency in rat livers by microarray analysis. *Biochem Pharmacol* **68**, 1465–1475.

Kiyosawa, N., Shiwaku, K., Hirode, M., Omura, K., Uehara, T., Shimizu, T., Mizukawa, Y., Miyagishima, T., Ono, A., Nagao, T. and Urushidani, T. (2006). Utilization of a one-dimensional score for surveying the chemical-induced changes in expression levels of multiple biomarker gene sets using a large-scale toxicogenomics database. *J Tox Sci* **31**, 433–448.

Kiyosawa, N., Uehara, T., Omura, K., Hirode, M., Shimizu, T., Mizukawa, Y., Gao, W., Ono, A., Miyagishima, T., Nagao, T. and Urushidani, T. (2007). Identification of glutathione depletion-responsive genes using phorone-treated rat liver. *J Tox Sci* in press.

Moggs, J. G., Tinwell, H., Spurway, T., Chang, H.-S., Pate, I., Lim, F. Le, Moore, D. J., Soames, A., Stuckey, R., Currie, R., Zhu, T., Kimber, I., Ashby, J. and Orphanides, G. (2004). Phenotypic Anchoring of Gene Expression Changes during Estrogen-Induced Uterine Growth. *Environ Health Perspect* **112**, 1589–1606.

Morishita, K., Mizukawa, Y., Kasahara, T., Okuyama, M., Takashima, K., Toritsuka, N. Miyagishima, T., Nagao, T. and Urushidani, T. (2006). Gene Expression Profile in Liver of Differing Ages of Rats after Single Oral Administration of Acetaminophen. *J. Tox Sci* **31**, 491–508.

Petit, S. (2004). Toxicogenomics in Risk Assessment: Communicating the Challenges. Environ *Health Perspect* **112**, A662.

Porter, M. W., Castle, A. L., Orr, M. S. and Mendrick, D. L. (2003). Predictive Toxicogenomics, in *An Introduction to Toxicogenomics*, M. E. Burczynski (Ed.), CRC Press, Boca Raton, FL, USA, pp. 225–260.

Takashima, K., Mizukawa, Y., Morishita, K., Okuyama M., Kasahara, T., Toritsuka, N., Miyagishima, T., Nagao, T. and Urushidani, T. (2006). Effect of the difference in vehicles on gene expression in the rat liver – analysis of the control data in the Toxicogenomics Project Database. *Life Sci* **78**, 2787–2796.

Tamura, K., Ono, A., Miyagishima, T., Nagao, T., and Urushidani, T. (2006a). Comparison of gene expression profiles among papilla, medulla and cortex in rat kidney. *J Tox Sci* **31**, 449–470.

Tamura, K., Ono, A., Miyagishima, T., Nagao, T. and Urushidani, T. (2006b). Profiling of gene expression in rat liver and rat primary cultured hepatocytes treated with peroxisome proliferators. *J Tox Sci* **31**, 471–490.

Tibshirani, R., Hastie, T., Narasimhan, B. and Chu, G. (2002). Diagnosis of multiple cancer types by shrunken centroids of gene expression. *Proc Natl Acad Sci USA* **99**, 6567–6572.

Ueda, H. R, Chen, W., Minami, Y., Honma, S., Honma, K., Iino, M. and Hashimoto, S. (2004). Molecular-timetable methods for detection of body time and rhythm disorders from single-time-point genome-wide expression profiles. *Proc Natl Acad Sci USA* **101**, 11227–11232.

Urushidani, T. and Nagao, T. (2005) Toxicogenomics: the Japanese initiative, in *Handbook of Toxicogenomics – Strategies and Applications*, J. Borlak (Ed.), Wiley-VCH, Weinhaim, Germany, pp. 623–631.

Wildsmith S. and Spence, F. (2003). Preparation and Utilization of Microarrays, in *An Introduction to Toxicogenomics*, M. E. Burczynski (Ed.), CRC Press, Boca Raton, *FL, USA*, pp. 3–16.

Available online at www.sciencedirect.com
ScienceDirect
Toxicology and Applied Pharmacology xx (2008) xxx – xxx
Toxicology and Applied Pharmacology
www.elsevier.com/locate/ytaap

Gene expression profiling in rat liver treated with compounds inducing phospholipidosis

Mitsuhiro Hirode [a,b], Atsushi Ono [b,c], Toshikazu Miyagishima [b], Taku Nagao [d], Yasuo Ohno [c], Tetsuro Urushidani [b,e,*]

[a] Pharmaceutical Research Division, Development Research Center, Takeda Pharmaceutical Company Limited, Yodogawa-ku, Osaka, 532-8686, Japan
[b] Toxicogenomics Project, National Institute of Biomedical Innovation, Ibaraki, Osaka, 567-0085, Japan
[c] National Institute of Health Sciences, Setagaya-ku, Tokyo 158-8501, Japan
[d] Food Safety Commission of Japan, Chiyoda-ku, Tokyo, 100-8989, Japan
[e] Department of Pathophysiology, Doshisha Women's College of Liberal Arts, Kyotanabe, Kyoto 610-0395, Japan

Received 27 October 2007; revised 14 January 2008; accepted 19 January 2008

Abstract

We have constructed a large-scale transcriptome database of rat liver treated with various drugs. In an effort to identify a biomarker for diagnosis of hepatic phospholipidosis, we extracted 78 probe sets of rat hepatic genes from data of 5 drugs, amiodarone, amitriptyline, clomipramine, imipramine, and ketoconazole, which actually induced this phenotype. Principal component analysis (PCA) using these probes clearly separated dose- and time-dependent clusters of treated groups from their controls. Moreover, 6 drugs (chloramphenicol, chlorpromazine, gentamicin, perhexiline, promethazine, and tamoxifen), which were reported to cause phospholipidosis but judged as negative by histopathological examination, were designated as positive by PCA using these probe sets. Eight drugs (carbon tetrachloride, coumarin, tetracycline, metformin, hydroxyzine, diltiazem, 2-bromoethylamine, and ethionamide), which showed phospholipidosis-like vacuolar formation in the histopathology, could be distinguished from the typical drugs causing phospholipidosis. Moreover, the possible induction of phospholipidosis was predictable by the expression of these genes 24 h after single administration in some of the drugs. We conclude that these identified 78 probe sets could be useful for diagnosis of phospholipidosis, and that toxicogenomics would be a promising approach for prediction of this type of toxicity.

Keywords: Phospholipidosis; Toxicogenomics; Rat; Liver; Principal component analysis

Introduction

The toxicogenomics project was a 5-year collaborative project by the National Institute of Biomedical Innovation (NIBIO), the National Institute of Health Science (NIHS), and 15 pharmaceutical companies in Japan that started in 2002 (Urushidani and Nagao, 2005). Its aim was to construct a large-scale toxicology database of transcriptome for prediction of toxicity of new chemical entities in the early stage of drug development. About 150 chemicals, mainly medicinal compounds, were selected, and gene expression in liver (also kidney in some cases) was comprehensively analyzed by using Affymetrix GeneChip®. In 2007, the project was finished and the whole system, consisting of the database, the analyzing system and the prediction system, was completed and named as TG-GATEs (Genomics Assisted Toxicity Evaluation System developed by the Toxicogenomics Project, Japan). The present mission is to identify potential biomarker gene lists useful for prediction or diagnosis of drug-induced hepato- and nephro-toxicity using this system.

In toxicity studies, phospholipidosis (PLsis) is often observed in various tissues including liver, kidney, and lung. PLsis is a lipid storage disease characterized by intracellular accumulation of phospholipids and the appearance of membranous lamellar inclusions known as lamellar bodies. Its pathogenesis has been thought to be the unbalance of phospholipid turnover. As for drug-induced PLsis, it is well known that cationic

* Corresponding author. Department of Pathophysiology, Doshisha Women's College of Liberal Arts, Kyotanabe, Kyoto 610-0395, Japan. Fax: +81 774 65 8689.
E-mail address: turushid@dwc.doshisha.ac.jp (T. Urushidani).

0041-008X/$ - see front matter © 2008 Elsevier Inc. All rights reserved.
doi:10.1016/j.taap.2008.01.036

Please cite this article as: Hirode, M., et al., Gene expression profiling in rat liver treated with compounds inducing phospholipidosis, Toxicol. Appl. Pharmacol. (2008), doi:10.1016/j.taap.2008.01.036

amphiphilic drugs (CADs), characterized by a hydrophobic ring structure and a hydrophilic side chain with a charged amine group have the potential to cause PLsis. Therefore, it has been postulated that drug-induced PLsis involves direct binding of CADs to phospholipids, subsequently creating a complex that is resistant to degradation by phospholipases (Reasor et al., 2006). There is also an observation that some CADs can cause PLsis by directly inhibiting phospholipase activity (Halliwell, 1997; Reasor et al., 2006). Although much effort has been done to establish the methods to predict PLsis of drugs (Tomizawa et al., 2006), sensitive diagnostic markers and effective prognostic markers are still desired.

In the present study, we selected PLsis in liver as a target phenotype, and tried to identify candidate biomarkers that enable the cell to discriminate chemicals with the potential to cause this phenotype for application of TG-GATEs.

Materials and methods

Compounds. Compounds used for the data analysis are listed in Table 1, in which the chemical name, abbreviation, dosage, administration route and vehicle used in the study are summarized.

Animal treatment. The experiments were carried out as previously described in the literature (Takashima et al., 2006). Male Crl:CD(SD) rats were purchased from Charles River Japan Inc., (Kanagawa, Japan) at 5-weeks of age. After a 7-day quarantine and acclimatization period, the animals were divided into groups of 5 animals using a computerized stratified random grouping method based on body weight for each age. The animals were individually housed in stainless-steel cages in a room that was lighted for 12 h (7:00–19:00) daily, ventilated with an air-exchange rate of 15 times per hour, and maintained at 21–25 °C with a relative humidity of 40–70%. Each animal was allowed free access to water and pellet food (CRF-1, sterilized by radiation, Oriental Yeast Co., Japan). Rats in each group were orally administered with various drugs suspended or dissolved either in 0.5% methylcellulose solution (MC) or corn oil according to their dispersibility, except for gentamicin and 2-bromoethylamine, which were dissolved in saline and administered intravenously. The animals were treated for 3, 7, 14 or 28 days and sacrificed 24 h after the last dosing. Blood samples were collected to a heparinized tube under ether anesthesia from the abdominal aorta after which the animals were euthanized.

The experimental protocols were reviewed and approved by the Ethics Review Committee for Animal Experimentation of the National Institute of Health Sciences.

Microarray analysis. After collecting the blood, the animals were euthanized by exsanguination from the abdominal aorta under ether anesthesia. An aliquot of the sample (about 30 mg) for RNA analysis was obtained from the left lateral lobe of the liver in each animal immediately after termination, kept in RNAlater® (Ambion, Austin, TX, USA) overnight at 4 °C, and then frozen at −80 °C until use. Liver samples were homogenized with the buffer RLT supplied in RNeasy Mini Kit (Qiagen, Valencia, CA, USA), and total RNA was isolated according to the manufacturer's instructions. Microarray analysis was conducted on 3 out of 5 samples for each group by using GeneChip® Rat Genome 230 2.0 Arrays (Affymetrix, Santa Clara, CA, USA), containing 31,042 probe sets. The procedure was conducted basically according to the manufacturer's instructions using Superscript Choice System (Invitrogen, Carlsbad, CA, USA) and T7-(dT)24-oligonucleotide primer (Affymetrix) for cDNA synthesis, cDNA Cleanup Module (Affymetrix) for purification, and BioArray High yield RNA Transcript Labeling Kit (Enzo Diagnostics, Farmingdale, NY, USA) for synthesis of biotin-labeled cRNA. Ten micrograms of fragmented cRNA was hybridized to a Rat Genome 230 2.0 Array for 18 h at 45 °C at 60 rpm, after which the array was washed and stained by streptavidin–phycoerythrin using Fluidics Station 400 (Affymetrix) and scanned by Gene Array Scanner (Affymetrix). The digital image files were processed by Affymetrix Microarray Suite version 5.0. Microarray image data were analyzed with GeneChip Operating Software (Affymetrix).

The digital image files were processed by Affymetrix Microarray Suite version 5.0 and the intensities were normalized for each chip by setting the mean intensity to 500 (per chip normalization).

Statistical analysis. In order to extract probe sets related to PLsis, we first employed gene expression data of rat liver treated with repeated administration for 3, 7, 14, and 28 days of AM, AMT, CPM, IMI and KC in our database, and they are known to cause PLsis, and in fact, the induction of this disease was confirmed in the present study.

After removing the probe sets with Affymetrix absent call in the whole 48 sample set ($N=3$ for 4 time points and 4 dose levels for one drug), differentially

Table 1
Compounds

Compound name	Abbreviation	Dose (dose level, mg/kg)			Administration route	Vehicle
		Low	Middle	High		
Amiodarone	AM	200/20*	600/60*	2000/200*	PO	MC
Amitriptyline	AMT	15	50	150	PO	MC
Clomipramine	CPM	10	30	100	PO	MC
Imipramine	IMI	10	30	100	PO	MC
Ketoconazole	KC	10	30	100	PO	MC
Chloramphenicol	CMP	100	300	1000	PO	MC
Chlorpromazine	CPZ	4.5	45/15*	150/45*	PO	MC
Gentamicin	GMC	10	30	100	IV	SA
Perhexiline	PH	15	50	150	PO	MC
Promethazine	PMZ	20	60	200	PO	MC
Tamoxifen	TMX	6	20	60	PO	CO
Carbon tetrachloride	CCl4	30	100	300	PO	CO
Coumarin	CMA	15	50	150	PO	CO
Tetracycline	TC	100	300	1000	PO	MC
Metformin	MFM	100	300	1000	PO	MC
Hydroxyzine	HYZ	10	30	100	PO	MC
Diltiazem	DIL	80	240	800	PO	MC
2-bromoethylamine	BEA	6/2*	20/6*	60/20*	IV	SA
Ethionamide	ETH	100/30*	300/100*	1000/300*	PO	MC

*: as single dose/repeated dose.
PO: peroral, IV: intravenous.
MC: 0.5 w/v% methylcellulose; SA: saline; CO: corn oil.

Please cite this article as: Hirode, M., et al., Gene expression profiling in rat liver treated with compounds inducing phospholipidosis, Toxicol. Appl. Pharmacol. (2008), doi:10.1016/j.taap.2008.01.036

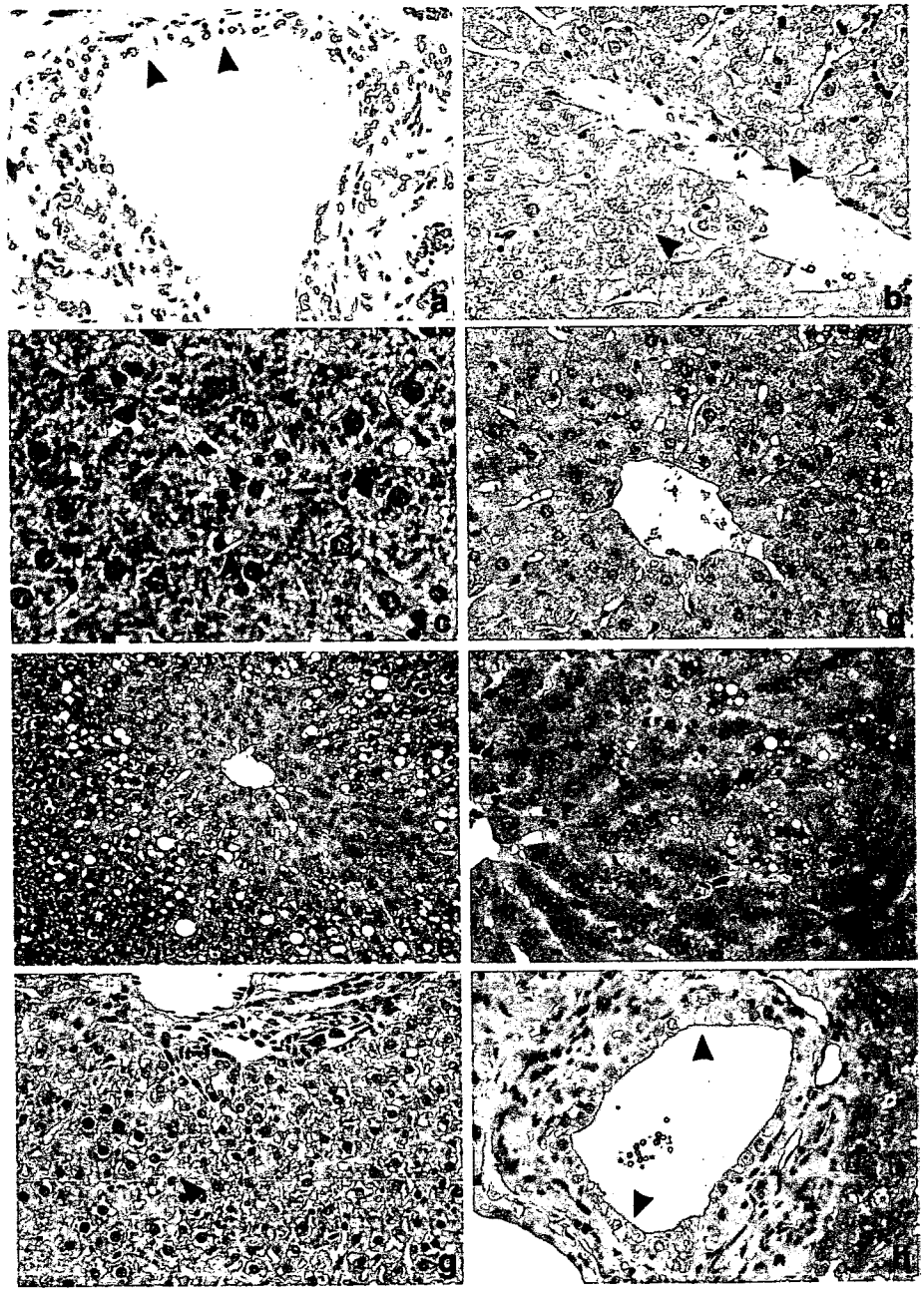

Q2 Fig. 1. Histopathology of rat liver treated with amiodarone, amitriptyline, clomipramine, imipramine, and ketoconazole. a–c. Amiodarone 200 mg/kg, 29th day. Vacuolations in the bile duct cell (a) in the hepatocyte (b) and in the Kupffer cell (c) are evident (arrowheads). d. Amitriptyline 150 mg/kg, 29th day. Vacuolation in the hepatocyte is evident. e. Clomipramine 100 mg/kg, 29th day. Vacuolation is noted in the midlobular hepatocytes. f–g. Imipramine 100 mg/kg, 29th day. Vacuolations in the hepatocyte (f) and in the Kupffer cell (g) are evident. h. Ketoconazole 100 mg/kg, 29th day. Vacuolation occurs exclusively in the bile duct (arrowheads).

expressed genes by the treatment were extracted by Welch's ANOVA ($p<0.05$) for the dose level at any time point. This procedure was continued for 4 time points and genes showing significant change, and any points were combined as PLsis responsive genes. In the next step, commonly mobilized genes among these 5 chemicals were selected.

Principal component analysis (PCA) of the GeneChip data was also performed using Spotfire DecisionSite.

Pathway and gene ontology (GO) analysis. The identified probe sets were subjected to analysis of Kyoto Encyclopedia of Genes and Genomes (KEGG) pathway and GO analysis by DAVID (Database for Annotation, Visualization, and Integrated Discovery; http://apps1.niaid.nih.gov/david/ using Fisher's exact test (Dennis et al., 2003). Level 5 analysis was adopted.

Results

Histopathological examination

The results of histopathological examination of 5 compounds (AM, AMT, CPM, IMI and KC) known to induce PLsis are shown in Fig. 1 and Table 2. For most cases, clear vacuolization was observed in the cytoplasm of hepatocytes, and this change tended to progress with dose and time. Vacuolation was also noted in Kupffer cell (AM, IMI) or bile duct (AM). In the case of KC, vacuolation occurred exclusively in the bile duct.

Please cite this article as: Hirode, M., et al., Gene expression profiling in rat liver treated with compounds inducing phospholipidosis, Toxicol. Appl. Pharmacol. (2008), doi:10.1016/j.taap.2008.01.036

Table 2
Histopathological findings

Compound	Findings	Time	Dose		
			Low	Middle	High
AM	Vacuolization, bile duct cell	3 h–4 day	–	–	–
		8 day	–	–	3/5(±)
		15 day	–	–	1/5(±), 4/5(+)
		29 day	–	–	4/4(+)
	Vacuolization, hepatocyte	3 h–8 day	–	–	–
		15 day	–	–	2/5(±)
		29 day	–	–	4/4(±)
	Vacuolization, Kupffer cell	3 h–8 day	–	–	–
		15 day	–	–	5/5(±)
		29 day	–	–	4/4(±)
AMT	Vacuolization, hepatocyte	3 h–4 day	–	–	–
		8 day	–	–	4/5(±)
		15 day	–	1/5(±)	5/5(+)
		29 day	–	1/5(±), 2/5(+)	1/3(+), 2/3(2+)
CPM	Vacuolization, hepatocyte	3 h–15 day	–	–	–
		29 day	–	–	1/5(±), 1/5(+)
IMI	Vacuolization, hepatocyte	3 h–4 day	–	–	–
		8 day	–	–	4/5(±)
		15 day	–	–	1/5(±), 2/5(+)
		29 day	–	2/5(±)	1/4(±), 3/4(+)
	Vacuolization, Kupffer cell	3 h–8 day	–	–	–
		15 day	–	–	3/5(±)
		29 day	–	–	–
KC	Vacuolization, bile duct cell	3 h–24 h	–	–	–
		4 day	–	–	5/5(+)
		8 day	–	–	5/5(+)
		15 day	–	1/5(+)	2/5(+), 3/5(2+)
		29 day	–	1/5(±), 4/5(+)	5/5(2+)
CMP	Abnormality	3 h–29 day	–	–	–
CPZ	Abnormality	3 h–29 day	–	–	–
GMC	Abnormality	3 h–29 day	–	–	–
PH	Abnormality	3 h–29 day	–	–	–
PMZ	Abnormality	3 h–29 day	–	–	–
TMX	Abnormality	3 h–29 day	–	–	–
CCl4	Degeneration, fatty, hepatocyte	3 h–9 h	–	–	–
		24 h	–	2/5(±)	1/5(±), 4/5(+)
		4 day	4/5(±), 1/5(+)	5/5(+)	1/5(±), 4/5(+)
		8 day	1/5(±), 4/5(+)	5/5(+)	4/5(+), 1/5(2+)
		15 day	1/5(±), 4/5(+)	5/5(+)	4/5(+), 1/5(2+)
		29 day	5/5(+)	4/5(+), 1/5(2+)	2/5(+), 2/5(2+), 1/5(3+)
CMA	Vacuolization, hepatocyte	3 h–8 day	–	–	–
		15 day	–	–	2/5(±), 1/5(+)
		29 day	–	–	5/5(+)
TC	Vacuolization, hepatocyte	3 h–8 day	–	–	–
		15 day	–	–	2/5(±)
		29 day	–	–	2/5(±)
MFM	Deposit, glycogen, hepatocyte	3 h–24 h	–	–	–
		4 day	–	2/5(±)	5/5(±)
		8 day	–	–	2/5(±)
		15 day	–	–	2/5(±)
		29 day	–	–	1/5(±)
HYZ	Vacuolization, hepatocyte	3 h–8 day	–	–	–
		15 day	–	–	2/5(±), 2/5(+)
		29 day	–	–	4/5(+), 1/5(2+)
DIL	Vacuolization, hepatocyte	3 h–4 day	–	–	–
		8 day	–	–	2/5(±)
		15 day	–	1/5(±)	5/5(±)
		29 day	–	4/5(±)	4/4(±)
BEA	Vacuolization, hepatocyte	3 h–8 day	–	–	–
		15 day	–	–	2/5(+)
		29 day	–	4/5(+)	4/5(+)
ETH	Vacuolization, hepatocyte	3 h–24 h	–	–	–
		4 day	–	4/5(+), 1/5(2+)	5/5(+)
		8 day	–	3/5(±), 2/5(+)	3/3(+)
		15 day	–	2/5(±), 3/5(+)	2/5(±), 3/5(+)
		29 day	–	2/5(+)	NA

–: not remarkable, ±: minimal, +: mild, 2+: moderate, 3+: severe, NA: not applicable.

Microarray data analysis

Differentially expressed genes with statistical significance were extracted from each of 5 representative drugs inducing PLsis, as described in the Materials and methods section. The numbers of extracted probe sets were 4915 for AM, 3565 for AMT, 1907 for CPM, 2339 for IMI, and 3482 for KC. We then selected the probe sets that were commonly changed in all compounds and 78 probe sets were obtained. The list of these probe sets is shown in Table 3. Based on gene ontology, the contents of genes related to carboxylic acid metabolism, electron transport, amino acid metabolism, amine catabolism, and nitrogen compound catabolism were significantly high (Table 4). Although not significant, 4 lipid biosynthesis-related genes were contained. This feature might reflect the cellular changes related to lipid metabolism in association with PLsis.

Principal component analysis (PCA)

Using the 78 probe sets extracted as above, PCA was performed on the 5 drugs inducing PLsis. As shown in Fig. 2,

Please cite this article as: Hirode, M., et al., Gene expression profiling in rat liver treated with compounds inducing phospholipidosis, Toxicol. Appl. Pharmacol. (2008), doi:10.1016/j.taap.2008.01.036

t3.1 Table 3
t3.2 List of 78 probe sets changed in 5 compounds inducing PLsis

t3.3	Probe set ID	Gene title	Gene symbol
t3.4	1367676_at	High mobility group box 2	Hmgb2
t3.5	1367819_at	Glutamate oxaloacetate transaminase 2, mitochondrial	Got2
t3.6	1368016_at	Peroxisomal *trans*-2-enoyl-CoA reductase	Pecr
t3.7	1368171_at	Lysyl oxidase	Lox
t3.8	1368213_at	P450 (cytochrome) oxidoreductase	Por
t3.9	1368275_at	Sterol-C4-methyl oxidase-like	Sc4mol
t3.10	1368403_at	Retinoblastoma-like 2	Rbl2
t3.11	1368467_at	Cytochrome P450, family 4, subfamily F, polypeptide 2	Cyp4f2
t3.12	1368520_at	Apolipoprotein A-IV	Apoa4
t3.13	1368618_at	Growth factor receptor bound protein 14	Grb14
t3.14	1368718_at	Aldehyde dehydrogenase family 1, subfamily A4	Aldh1a4
t3.15	1368778_at	Solute carrier family 6 (neurotransmitter transporter, taurine), member 6	Slc6a6
t3.16	1368905_at	Carboxylesterase 2 (intestine, liver)	Ces2
t3.17	1368931_at	SH3-domain GRB2-like 3	Sh3gl3
t3.18	1368977_a_at	Fractured callus expressed transcript 1	Fxc1
t3.19	1369275_s_at	Cytochrome P450 IIA1 (hepatic steroid hydroxylase IIA1) gene	Cyp2a1
t3.20	1369737_at	cAMP responsive element modulator	Crem
t3.21	1369850_at	UDP-glucuronosyltransferase 2 family, polypeptide A1	Ugt2a1
t3.22	1370004_at	H2A histone family, member Y	H2afy
t3.23	1370054_at	Cyclin-dependent kinase inhibitor 2C (p18, inhibits CDK4)	Cdkn2c
t3.24	1370375_at	Glutaminase 2 (liver, mitochondrial)	Gls2
t3.25	1370583_s_at	ATP-binding cassette, subfamily B (MDR/TAP), member 1	Abcb1
t3.26	1370613_s_at	UDP glycosyltransferase 1 family, polypeptide A1	Ugt1a1
t3.27	1370698_at	Liver UDP-glucuronosyltransferase, phenobarbital-inducible form liver	Udpgtr2
t3.28	1371076_at	Cytochrome P450, family 2, subfamily b, polypeptide 15	Cyp2b15
t3.29	1371089_at	Transcribed locus	–
t3.30	1371412_a_at	Neuronal regeneration related protein	Nrep
t3.31	1371546_at	Similar to TR4 orphan receptor-associated protein TRA16	LOC361128
t3.32	1371680_at	Similar to gamma-aminobutyric acid (GABA(A)) receptor-associated protein-like 1	LOC683917
t3.33	1371809_at	Mitochondrial ribosomal protein S18B	Mrps18b
t3.34	1371875_at	Mannosidase, beta A, lysosomal	Manba
t3.35	1372056_at	CKLF-like MARVEL transmembrane domain containing 6	Cmtm6
t3.36	1372124_at	Eukaryotic translation initiation factor 4B	Eif4b
t3.37	1372181_at	Similar to expressed sequence AA408877	RGD1308513
t3.38	1372479_at	Transcribed locus, moderately similar to NP_064456.1 fibrinogen, beta polypeptide [*Rattus norvegicus*]	–
t3.39	1372602_at	Similar to genethonin 1	RGD1311800
t3.40	1372885_at	Transcribed locus	–
t3.41	1373015_at	Ring finger protein 11 (predicted)	Rnf11_predicted
t3.42	1373626_at	Transcribed locus	–
t3.43	1373823_at	Similar to cyclin-dependent kinases regulatory subunit 2 (CKS-2) (predicted)	RGD1562047_predicted
t3.44	1373924_at	Similar to C530044N13Rik protein	RGD1306568
t3.45	1373970_at	Similar to RIKEN cDNA 9230117N10	RGD1311155
t3.46	1374531_at	Transcribed locus	–
t3.47	1374953_at	Similar to CG12279-PA	LOC500420
t3.48	1375423_at	MAX-like protein X	Mlx
t3.49	1375637_at	Similar to RIKEN cDNA 1110003E01	RGD1311122
t3.50	1375909_at	Similar to glutathione transferase GSTM7-7	MGC108896
t3.51	1377019_at	Transcribed locus	–
t3.52	1378016_at	Echinoderm microtubule associated protein-like 4 (predicted)	Eml4_predicted
t3.53	1380254_at	Transcribed locus, moderately similar to NP_079928.1 general transcription factor III A [*Mus musculus*]	–
t3.54	1384169_a_at	Vav2 oncogene (predicted)	Vav2_predicted
t3.55	1386857_at	Stathmin 1	Stmn1
t3.56	1386917_at	Pyruvate carboxylase	Pc
t3.57	1387006_at	Rat senescence marker protein 2A gene, exons 1 and 2	Smp2a
t3.58	1387022_at	Aldehyde dehydrogenase family 1, member A1	Aldh1a1
t3.59	1387031_at	Endoplasmic reticulum protein 29	Erp29
t3.60	1387093_at	Solute carrier organic anion transporter family, member 1a4	Slco1a4
t3.61	1387094_at	Solute carrier organic anion transporter family, member 1a4	Slco1a4
t3.62	1387109_at	P450 (cytochrome) oxidoreductase	Por
t3.63	1387118_at	Cytochrome P450, family 3, subfamily a, polypeptide 1	Cyp3a1
t3.64	1387203_at	Glucokinase regulatory protein	Gckr

(continued on next page)

Please cite this article as: Hirode, M., et al., Gene expression profiling in rat liver treated with compounds inducing phospholipidosis, Toxicol. Appl. Pharmacol. (2008), doi:10.1016/j.taap.2008.01.036

Table 3 (*continued*)

Probe set ID	Gene title	Gene symbol
1387223_at	Aminoadipate aminotransferase	Aadat
1387307_at	Histidine ammonia lyase	Hal
1387511_at	Cytochrome P450 IIA1 (hepatic steroid hydroxylase IIA1) gene	Cyp2a1
1387665_at	Betaine-homocysteine methyltransferase	Bhmt
1387669_a_at	Epoxide hydrolase 1, microsomal	Ephx1
1387759_s_at	UDP glycosyltransferase 1 family, polypeptide A1	Ugt1a1
1387793_at	Transcribed locus, strongly similar to NP_075738.1 yippee-like 1 [*Mus musculus*]	–
1388212_a_at	RT1 class Ib, locus S3	RT1-S3
1388348_at	Transcribed locus	–
1388425_at	Similar to RIKEN cDNA D130038B21	RGD1305890
1388874_at	Metastasis suppressor 1 (predicted)	Mtss1_predicted
1389319_at	Similar to endoplasmic reticulum-Golgi intermediate compartment protein 1 (ER-Golgi intermediate compartment 32 kDa protein) (ERGIC-32)	LOC287177
1389557_at	Testis expressed gene 261	Tex261
1389986_at	CDNA clone IMAGE:7321089	–
1390455_at	Abhydrolase domain containing 2 (predicted)	Abhd2_predicted
1398754_at	Ubiquitin A-52 residue ribosomal protein fusion product 1	Uba52
1398848_at	Suppression of tumorigenicity 13	St13

treated samples were dose-dependently separated to form clusters from controls, mainly toward the direction of PC1 (contribution rate: 34.8%). In order to examine the time-dependency, all the samples were aligned on a one dimensional graph of PC1 (Fig. 3). It appears that the PC1 value generally increased with time as well as with a dose of these drugs. In case of KC, time- and dose-dependency were obscure, although the treated group clearly formed a cluster separated from the control cluster. Of the genes contributing to PC1, those with high eigenvector value were listed in Table 5. We noticed that the top 4 genes are cytochrome oxidoreductase, sterol-C4-methy oxidase-like, aldehyde dehydrogenase 1A4, and carboxylesterase 2, which are all involved in lipid metabolism.

Distinction of 6 compounds reported to induce PLsis with no abnormality in present histopathological examination

In a survey of the literature, in addition to the 5 drugs above, 6 more drugs, i.e., CMP, CPZ, GMC, PH, PMZ, and TMX in our database, are reported to induce PLsis, but no such histopathological abnormalities were confirmed in the present examination. We then applied PCA using the 78 probe sets on these 6 drugs and we show the results in Fig. 4 as a one dimensional graph with PC1. It was revealed that these 6 drugs were also separated from control clusters the same way as the 5 typical drugs inducing PLsis. Of these, some drugs such as CPZ, GMC and PH, did not change their position very much, but their extent was roughly equivalent to that of KC.

Distinction of 8 compounds showing pathological changes similar to PLsis

When examination by light microscope of HE-stained specimens is performed, we sometimes encounter a phenotype (not PLsis but another pathological change), such as lipidosis, deposition of glycogen, or hydropic degeneration, and they are quite difficult to distinguish from each other. In our database, we identified 8 drugs (CCL4, CMA, TC, MFM, HYZ, DIL, BEA, and ETH) showing such pathological changes in liver. The histopathological description of each was as follows: CCL4: "degeneration, fatty, hepatocyte"; CMA, TC, HYZ, DIL, BEA, ETH: "vacuolization, hepatocyte"; and MFM: "deposit, glycogen, hepatocyte". To examine the efficiency of the 78 probe sets, PCA was applied to these 8 pseudo-positive compounds.

As shown in Fig. 5, most of the treated samples stayed in the position close to that of the control samples. Exceptionally, HYZ and DIL formed separate clusters from the controls, as 5 standard compounds inducing PLsis.

Possible distinction of the samples 24 h after a one time dosage

The above results clearly suggested that the list of extracted 78 probe sets was a useful diagnostic marker for PLsis in rat liver. The next question is whether the list works as a prognostic marker for PLsis. To examine this possibility, we performed PCA using the list for the gene expression profile 24 h after the single dose, and practically no pathological changes had occurred at that time. As shown in Fig. 6 left, AM 20, 60, and 200 mg/kg had a high PC1 value in repeated administration for 3 days or more, whereas that in the single dose group was close to the cluster of the control group. Then we additionally performed single dose experiments using higher doses, i.e., 200,

Table 4
GO analysis of identified 78 probe sets

Term	Count	Percent	*P*-value
Carboxylic acid metabolism	10	11.5	1.90E–04
Electron transport	6	6.9	1.20E–02
Amino acid metabolism	5	5.7	1.80E–02
Amine catabolism	3	3.4	3.20E–02
Nitrogen compound catabolism	3	3.4	3.40E–02
Lipid biosynthesis	4	4.6	6.10E–02

Please cite this article as: Hirode, M., et al., Gene expression profiling in rat liver treated with compounds inducing phospholipidosis, Toxicol. Appl. Pharmacol. (2008), doi:10.1016/j.taap.2008.01.036

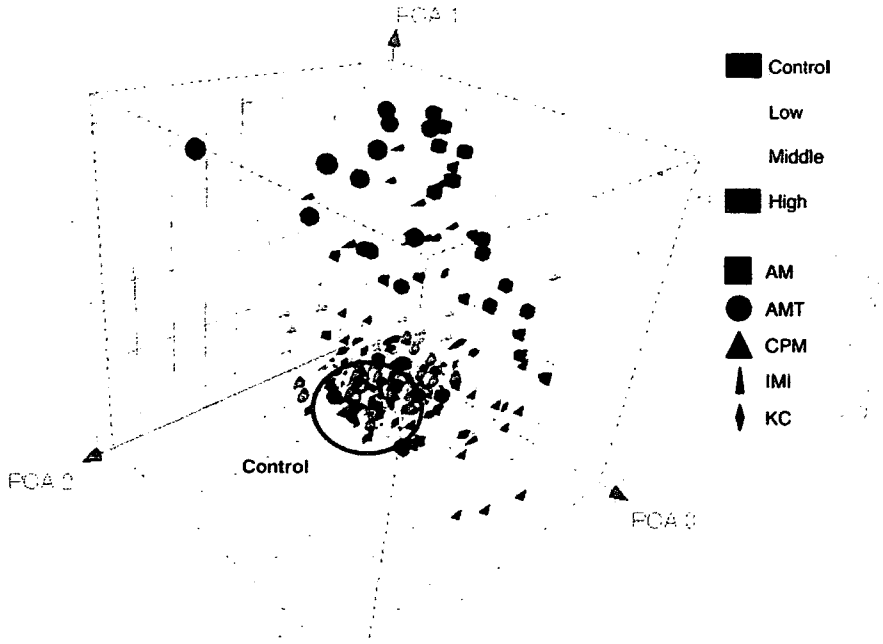

Fig. 2. Principal component analysis of gene expression profiles of amiodarone (AM), amitriptyline (AMT), clomipramine (CPM), imipramine (IMI), and ketoconazole (KC) that induced phospholipidosis in liver in the present study using the commonly mobilized 78 probe sets. Results are expressed as a three dimensional figure with PC1, 2, and 3. Treated samples were dose-dependently separated from the cluster of controls (circled by a blue line), mainly toward the direction of PC1 (contribution rate: 34.8%). For simplicity, rats receiving the same dose with different durations (3, 7, 14 and 28 days, N=3 for each; 12 total) were expressed by the same symbol.

600, and 2000 mg/kg of AM (Fig. 6, right). It was revealed that the group receiving a single dose of 2000 mg/kg AM clustered at a position clearly higher than controls with equivalent PCA1 values receiving a repeated dose of 200 mg/kg for 3 days. In the case of CPZ, the samples at 24 h after the 45 mg/kg single dosing were clearly separated from control samples to an extent more than that of the repeated dose samples (Fig. 7). We then performed additional single dose experiments using 45 and 150 mg/kg CPZ. It was clear from Fig. 7 that 150 mg/kg CPZ showed a higher PC1 value than the 45 mg/kg group.

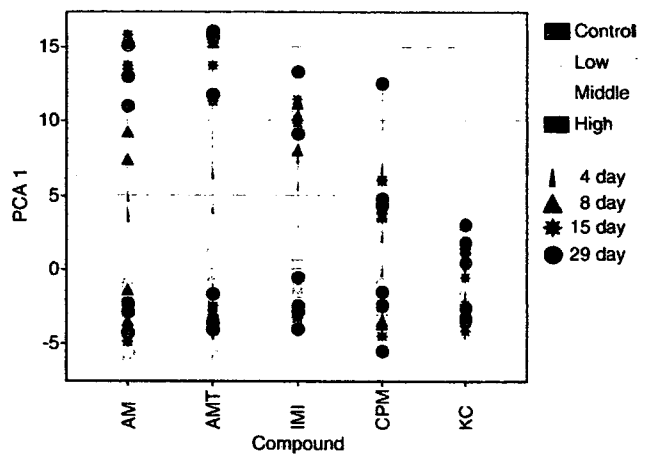

Fig. 3. Principal component analysis the same as Fig. 2 but with one dimensional expression using principal component 1. For each drug, each individual rat is depicted by a symbol with a different color and shape as shown on the right panel.

Discussion

PLsis has been one of the main concerns in the course of drug development, since its appropriate biomarkers are lacking, especially in the clinical field. In order to assess PLsis, a variety of in vitro methodologies have recently been described, e.g., using fluorescent dyes (Casartelli et al., 2003) or fluorescently labeled phospholipids (Kasahara et al., 2006, Nioi et al., 2007) in cell culture. However, these assay systems only work to estimate the potential of PLsis, but not to tell its mechanism and thus they do not help in deciding whether to go ahead or to switch to other candidates in the development process. One promising strategy would be a toxicogenomics approach. Sawada et al. (2005) recently identified a panel of 17 genes where the expression profile would predict the possibility of PLsis using HepG2 cells. This result was further transferred to a 96-well plate to attain a high throughput genomics-based platform (Sawada et al., 2006). Although the advantage of the genomics-based strategy was postulated to elucidate the background toxicological mechanism, the gene expression changes have not been related to the pathophysiological aspects of PLsis. It has been suggested that PLsis is induced by the disturbance of lipid turnover, i.e., excess of lipid biosynthesis, inhibition of lipid degradation enzymes (especially lysosomal phospholipase A2), and inhibition of lipid transporter in lysosomes. In the case of drug-induced PLsis, most of it has been attributed to the inhibition of phospholipase

Please cite this article as: Hirode, M., et al., Gene expression profiling in rat liver treated with compounds inducing phospholipidosis, Toxicol. Appl. Pharmacol. (2008), doi:10.1016/j.taap.2008.01.036

Table 5
List of 28 probe sets contributing PC1

Ranking	Probe set ID	Gene title	Eigenvalue
1	1368905_at	Carboxylesterase 2 (intestine, liver)	0.165043
2	1387759_s_at	UDP glycosyltransferase 1 family, polypeptide A1	0.163056
3	1387022_at	Aldehyde dehydrogenase family 1, member A1	0.158847
4	1371076_at	Cytochrome P450, family 2, subfamily b, polypeptide 15	0.156238
5	1387118_at	Cytochrome P450, family 3, subfamily a, polypeptide 1	0.153634
6	1387109_at	P450 (cytochrome) oxidoreductase	0.152900
7	1371089_at	Transcribed locus	0.152322
8	1368718_at	Aldehyde dehydrogenase family 1, subfamily A4	0.147161
9	1370613_s_at	UDP glycosyltransferase 1 family, polypeptide A1	0.145621
10	1368977_a_at	Fractured callus expressed transcript 1	0.145613
11	1370583_s_at	ATP-binding cassette, subfamily B (MDR/TAP), member 1	0.145395
12	1380254_at	Transcribed locus, moderately similar to NP_079928.1 general transcription factor III A [*Mus musculus*]	0.145244
13	1387669_a_at	Epoxide hydrolase 1, microsomal	0.144549
14	1370698_at	Liver UDP-glucuronosyltransferase, phenobarbital-inducible form liver	0.143250
15	1368213_at	P450 (cytochrome) oxidoreductase	0.142376
16	1375423_at	MAX-like protein X	0.135972
17	1387094_at	Solute carrier organic anion transporter family, member 1a4	0.131073
18	1372602_at	Similar to genethonin 1	0.129514
19	1369850_at	UDP-glucuronosyltransferase 2 family, polypeptide A1	0.129217
20	1368275_at	Sterol-C4-methyl oxidase-like	0.129122
21	1371875_at	Mannosidase, beta A, lysosomal	0.128496
22	1372479_at	Transcribed locus, moderately similar to NP_064456.1 fibrinogen, beta polypeptide [*Rattus norvegicus*]	0.127711
23	1387093_at	Solute carrier organic anion transporter family, member 1a4	0.127266
24	1371809_at	Mitochondrial ribosomal protein S18B	0.126952
25	1384169_a_at	Vav2 oncogene (predicted)	0.125901
26	1375909_at	Similar to glutathione transferase GSTM7-7	0.125538
27	1373924_at	Similar to C530044N13Rik protein	0.122349
28	1371680_at	Similar to gamma-aminobutyric acid (GABA(A)) receptor-associated protein-like 1	0.117093

activity either through the generation of CAD-phospholipid complexes or by direct inhibition of phospholipase activity (Reasor et al., 2006). It is clearly necessary to elucidate how these changes are reflected in gene expression in order to make a prediction based on the genomics approach.

In the present study, we extracted 78 genes commonly mobilized in the 5 typical PLsis-inducing drugs, i.e., AM (Honegger et al., 1993), AMT (Drenckhahn et al., 1976), CPM (Xia et al., 2000), IMI (Drew et al., 1981; Hansson et al., 1997) and KC (Whitehouse et al., 1994). By PCA, we used these genes to successfully separate the high risk group from the low risk ones, except for KC, which showed relatively obscure separation. This is reasonable, as the histopathology of KC only causes changes

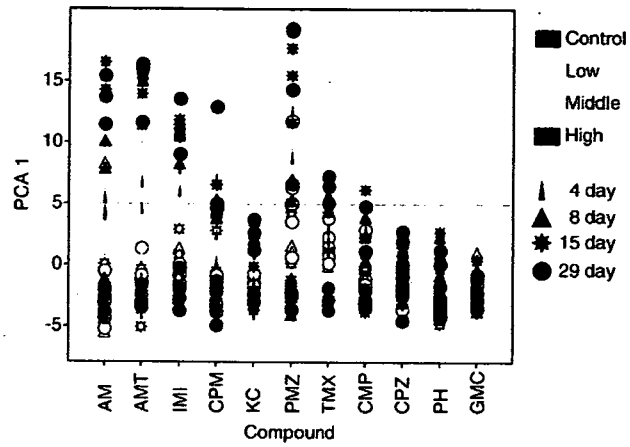

Fig. 4. Principal component analysis of gene expression profiles of 6 compounds reported to induce PLsis but no abnormality in present histopathological examination, i.e., chloramphenicol (CMP), chlorpromazine (CPZ), gentamicin (GMC), perhexiline (PH), promethazine (PMZ), and tamoxifen (TMX) using the commonly mobilized 78 probe sets. For comparison, 5 compounds shown in Figs. 2 and 3, amiodarone (AM), amitriptyline (AMT), clomipramine (CPM), imipramine (IMI), and ketoconazole (KC), are also included. Results are expressed as a one dimensional figure with PC1 (contribution rate: 34.8%). For each drug, each individual rat is depicted by a symbol with a different color and shape as shown on the right panel.

in the bile duct cells, in contrast to the other 4 drugs that elicit changes in the hepatocytes.

CMP (Joshi et al., 1989), CPZ (Kodavanti et al., 1990), GMC (Kacew, 1987), PH (Pessayre et al., 1979), PMZ (Joshi et al., 1989) and TMX (Reasor and Kacew, 2001) have also been reported to induce PLsis, but we could not detect PLsis in liver by histopathological examinations in the present study. This is not surprising when the sensitivity of detection by histopathology is

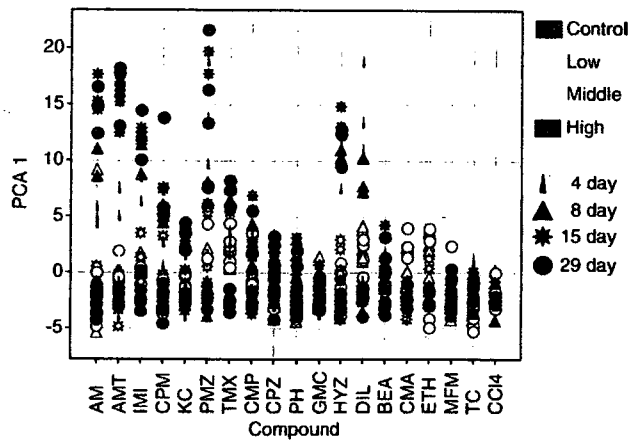

Fig. 5. Principal component analysis of gene expression profiles of 8 compounds showing pathological changes similar to PLsis, i.e., carbon tetrachloride (CCL4), coumarin (CMA), tetracycline (TC), metformin (MFM), hydroxyzine (HYZ), diltiazem (DIL), 2-bromoethylamine (BEA), and ethionamide (ETH), using the commonly mobilized 78 probe sets. For comparison, the 5 compounds shown in Figs. 2 and 3, amiodarone (AM), amitriptyline (AMT), clomipramine (CPM), imipramine (IMI) and ketoconazole (KC), and the 6 compounds in Fig. 4, chloramphenicol (CMP), chlorpromazine (CPZ), gentamicin (GMC), perhexiline (PH), promethazine (PMZ), and tamoxifen (TMX) are also included. Results are expressed as a one dimensional figure with PC1 (contribution rate: 34.8%). For each drug, each individual rat is depicted by a symbol with a different color and shape as shown on the right panel.

Please cite this article as: Hirode, M., et al., Gene expression profiling in rat liver treated with compounds inducing phospholipidosis, Toxicol. Appl. Pharmacol. (2008), doi:10.1016/j.taap.2008.01.036

considered. In particular, our dose setting for the database was based on preliminary experiments of repeated dosing for 7 days with the proviso that all animals are to survive for 28 days. This sometimes brings about a situation that the dose level is too low for certain phenotypes. This point is particularly problematic when biomarker gene lists are to be extracted based on the actually observed phenotype. Of these 6 drugs, we could judge CMP, PMZ and TMX as positive by PCA using the present marker genes, whereas CPZ, GMC and PH were weakly positive or almost negative. These observations could be due to a feature of the marker genes: a considerable part of them actually reflects the occurring pathological changes, namely, they work as diagnostic markers. The fact that some of the drugs could be judged as positive suggested that their diagnosis from marker genes was more sensitive than pathological examination.

GMC has been reported to cause PLsis in kidney tissue and this is associated with renal tubular toxicity (Kaloyanides and Pastoriza-Munoz, 1980; Laurent et al., 1990). This might be attributed to its negative judgment for PLsis in liver since potential biochemical/pathological changes would mainly occur in kidney. It is of interest to investigate the gene expression changes in kidney, but another set of genes would be necessary to make a precise diagnosis for PLsis in kidney.

PH was selected as a PLsis-positive drug but appeared to be negative or a very weak positive in the present study using rats. This might be due to the species difference in the drug metabolism since the risk of PH-induced liver injury is higher in individuals with the P450IID6 poor-metabolizer phenotype (Morgan et al., 1984, Pessayre and Larrey, 1988).

Some compounds show morphological changes similar to PLsis. In our database, there are 8 such compounds, i.e., CCL4, CMA, TC, MFM, HYZ, DIL, BEA, and ETH. Of these, CCL4 (Weber et al., 2003), TC (Fréneaux et al., 1988), BEA (Thiele-

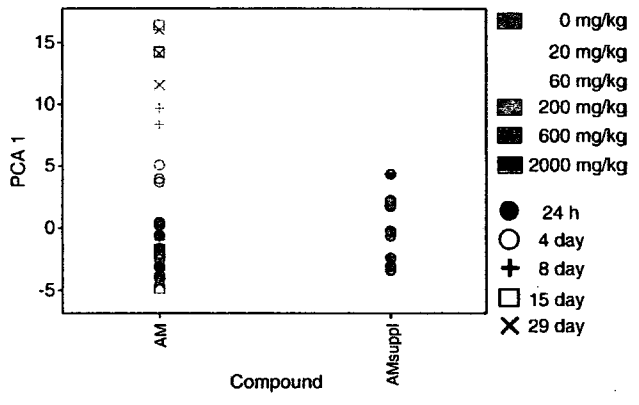

Fig. 6. Principal component analysis of gene expression profiles of amiodarone. Results are expressed as a one dimensional figure with PC1 (contribution rate: 34.8%). Each individual rat is depicted by a symbol with a different color and shape as shown on the right panel. On the left, the data of 24 h after a single treatment (filled symbols) are added to the data for repeated treatment (open or line symbols) shown in the previous figures. Note that the PC1 value of a single dose is low even at the highest dose, 200 mg/kg (red filled circle) compared with the repeated dose (red open or line symbols). On the left, a supplemental higher dose experiment was performed. Note that the higher dose (600 mg/kg, dark red; 2000 mg/kg, black) showed a dose-dependent increase in PC1 reaching to a value of 200 mg/kg at 4 days.

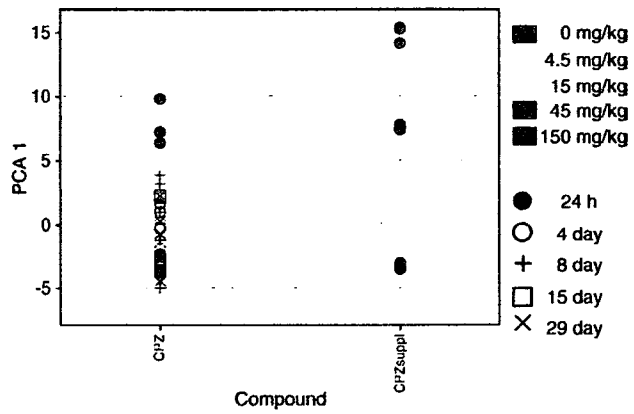

Fig. 7. Principal component analysis of gene expression profiles of chlorpromazine. Results are expressed as a one dimensional figure with PC1 (contribution rate: 34.8%). Each individual rat is depicted by a symbol with a different color and shape as shown on the right panel. On the left, the data of 24 h after a single treatment (filled symbols) are added to the data for repeated treatment (open or line symbols) shown in the previous figures. In contrast to the results in Fig. 6, the single dose of 45 mg/kg (red filled circle) gave higher PC1 values compared with samples of repeated dosing. On the left, a supplemental higher dose (150 mg/kg) experiment was performed in addition to 45 mg/kg. Note that the higher dose (dark red) showed even higher PC1 values.

mann et al., 1999), and ETH (Kuntz et al., 1968, Inouye et al., 1973) are reported to show morphology associated with a change in the lipid storage, i.e., lipidosis or steatosis. CMA is known to cause hepatic necrosis (Lake, 1984) and MFM induces a deposition of glycogen. These drugs, which do not induce PLsis, could be separated from the clusters of PLsis-inducing ones by PCA using the extracted genes. As for HYZ (Hruban et al., 1972), classified as PLsis-positive by PCA in this study, there is a recent report that it actually induced PLsis (Pelletier et al., 2007). The only exception was the case of DIL, which showed vacuolation in hepatocytes and was not considered as PLsis, but was classified as positive by PCA. Reviewing the PCA (Fig. 5) however, it is noticeable that the time-dependent changes in the PC1 value are exceptionally different from other drugs such that the value transiently increases with the peak at 4 days, then decreases with time and returns to negative at the 15th day. It is necessary to elucidate the mechanism of the unique change observed in DIL, but it appears that this drug is to be judged as pseudo-positive by the present criteria.

One important question is whether the toxicogenomics approach enables not only diagnosis but also prognosis of PLsis. The results shown in Figs. 6 and 7 provide a clue. In general, it appears to be difficult to predict the potential of PLsis occurring 14 days or later with repeated administration with the data for single dosing, but it could be possible when a high enough dose is applied in some cases. We are presently in a preliminary stage, but we hope to establish a really useful marker gene set in a future study with a strategic protocol, which can predict PLsis in liver by single dosing within 24 h. In the present study, we exclusively worked on liver where enough gene expression data are stored in our database. As PLsis occurs in organs other than liver, it is of interest to apply the present strategy to other organs such as kidney whose transcriptome data are now accumulating in our database.

Please cite this article as: Hirode, M., et al., Gene expression profiling in rat liver treated with compounds inducing phospholipidosis, Toxicol. Appl. Pharmacol. (2008), doi:10.1016/j.taap.2008.01.036

There remain many problems to be solved in the present system, such as the improvement of accuracy and sensitivity, the elucidation of the functions of the genes in the list (especially in the pathological mechanism of PLsis), the breakthrough species difference, and so on. However, the presently identified 78 probe sets from gene expression data stored in TG-GATEs have provided a powerful starting tool.

Acknowledgment

This work was supported in part by the grants from Ministry of Health, Labour and Welfare of Japan, H14-001-Toxico.

References

Casartelli, A., Bonato, M., Cristofori, P., Crivellente, F., Dal Negro, G., Masotto, I., Mutinelli, C., Valko, K., Bonfante, V., 2003. A cell-based approach for the early assessment of the phospholipidogenic potential in pharmaceutical research and drug development. Cell Biol. Toxicol. 19, 161–176.

Dennis Jr., G., Sherman, B.T., Hosack, D.A., Yang, J., Gao, W., Lane, H.C., Lempicki, R.A., 2003. DAVID: database for annotation, visualization, and integrated discovery. Genome Biol. 4, P3.

Drenckhahn, D., Kleine, L., Lullmann-Rauch, R., 1976. Lysosomal alterations in cultured macrophages exposed to anorexigenic and psychotropic drugs. Lab. Invest. 35, 116–123.

Drew, R., Siddik, Z.H., Mimnaugh, E.G., Gram, T.E., 1981. Species and dose differences in the accumulation of imipramine by mammalian lungs. Drug Metab. Dispos. 9, 322–326.

Fréneaux, E., Labbe, G., Letteron, P., The Le Dinhi, Degott, C., Genève, J., Larrey, D., Pessayre, D., 1988. Inhibition of the mitochondrial oxidation of fatty acids by tetracycline in mice and in man: possible role in microvesicular steatosis induced by this antibiotic. Hepatology 8, 1056–1062.

Halliwell, W.H., 1997. Cationic amphiphilic drug-induced phospholipidosis. Toxicol. Pathol. 25, 53–60.

Hansson, A.L., Xia, Z., Berglund, M.C., Bergstrand, A., Depierre, J.W., Nässberger, L., 1997. Reduced cell survival and morphological alterations induced by three tricyclic antidepressants in human peripheral monocytes and lymphocytes and in cell lines derived from these cell types. Toxicol. In Vitro 11, 21–31.

Honegger, U.E., Zuehlke, R.D., Scuntaro, I., Schaefer, M.H., Toplak, H., Wiesmann, U.N., 1993. Cellular accumulation of amiodarone and desethylamiodarone in cultured human cells. Consequences of drug accumulation on cellular lipid metabolism and plasma membrane properties of chronically exposed cells. Biochem. Pharmacol. 45, 349–356.

Hruban, Z., Slesers, A., Hopkins, E., 1972. Drug-induced and naturally occurring myeloid bodies. Lab. Invest. 27, 62–70.

Inouye, B., Yoshimura, N., Wachi, T., 1973. Experimental studies on the mechanism of fatty liver formation induced by ethionamide. V. Liver and serum total cholesterol in ethionamide-administered rats. Kekkaku 48, 71–74.

Joshi, U.M., Rao, P., Kodavanti, S., Lockard, V.G., Mehendale, H.M., 1989. Fluorescence studies on binding of amphiphilic drugs to isolated lamellar bodies: relevance to phospholipidosis. Biochim. Biophys. Acta 1004, 309–320.

Kacew, S., 1987. Cationic amphiphilic drug-induced renal cortical lysosomal phospholipidosis: an in vivo comparative study with gentamicin and chlorphentermine. Toxicol. Appl. Pharmacol. 91, 469–746.

Kaloyanides, G.J., Pastoriza-Munoz, E., 1980. Aminoglycoside nephrotoxicity. Kidney Int, 18, 571–582.

Kasahara, T., Tomita, K., Murano, H., Harada, T., Tsubakimoto, K., Ogihara, T., Ohnishi, S., Kakinuma, C., 2006. Establishment of an in vitro high-throughput screening assay for detecting phospholipidosis-inducing potential. Toxicol. Sci. 90, 133–141.

Kodavanti, U.P., Lockard, V.G., Mehendale, H.M., 1990. In vivo toxicity and pulmonary effects of promazine and chlorpromazine in rats. J. Biochem. Toxicol. 5, 245–251.

Kuntz, E., Liehr, H., Pfingst, W., 1968. Toxic liver damage due to ethionamide. Ger. Med. Mon. 13, 599–602.

Lake, B.G., 1984. Investigations into the mechanism of coumarin-induced hepatotoxicity in the rat. Arch. Toxicol. Suppl. 7, 16–29.

Laurent, G., Kishore, B.K., Tulkens, P.M., 1990. Aminoglycoside-induced renal phospholipidosis and nephrotoxicity. Biochem. Pharmacol. 40, 2383–2392.

Morgan, M.Y., Reshef, R., Shah, R.R., Oates, N.S., Smith, R.L., Sherlock, S., 1984. Impaired oxidation of debrisoquine in patients with perhexiline liver injury. Gut 25, 1057–1064.

Nioi, P., Perry, B.K., Wang, E.J., Gu, Y.Z., Snyder, R.D., 2007. In vitro detection of drug-induced phospholipidosis using gene expression and fluorescent phospholipid based methodologies. Toxicol. Sci. 99, 162–173.

Pelletier, D.J., Gehlhaar, D., Tilloy-Ellul, A., Johnson, T.O., Greene, N., 2007. Evaluation of a published in silico model and construction of a novel bayesian model for predicting phospholipidosis inducing potential. J. Chem. Inf. Model 47, 1196–1205.

Pessayre, D., Bichara, M., Degott, C., Potet, F., Benhamou, J.P., Feldmann, G., 1979. Perhexiline maleate-induced cirrhosis. Gastroenterol. 76, 170–177.

Pessayre, D., Larrey, D., 1988. Acute and chronic drug-induced hepatitis. Baillieres Clin. Gastroenterol. 2, 385–422.

Reasor, M.J., Kacew, S., 2001. Drug-induced phospholipidosis: are there functional consequences? Exp. Biol. Med. 226, 825–830.

Reasor, M.J., Hastings, K.L., Ulrich, R.G., 2006. Drug-induced phospholipidosis: issues and future directions. Expert Opin. Drug Saf. 5, 567–583.

Sawada, H., Takami, K., Asahi, S., 2005. A toxicogenomic approach to drug-induced phospholipidosis: analysis of its induction mechanism and establishment of a novel in vitro screening system. Toxicol. Sci. 83, 282–292.

Sawada, H., Taniguchi, K., Takami, K., 2006. Improved toxicogenomic screening for drug-induced phospholipidosis using a multiplexed quantitative gene expression ArrayPlate assay. Toxicol. In Vitro 20, 1506–1513.

Takashima, K., Mizukawa, Y., Morishita, K., Okuyama, M., Kasahara, T., Toritsuka, N., Miyagishima, T., Nagao, T., Urushidani, T., 2006. Effect of the difference in vehicles on gene expression in the rat liver-analysis of the control data in the Toxicogenomics Project Database. Life Sci. 78, 2787–2796.

Thielemann, L.E., Bosco, C., Rodrigo, R., Orellana, M., Videla, L.A., 1999. Effects of bromoethylamine on antioxidant capacity, lipid peroxidation, and morphological characteristics of rat liver. J. Biochem. Mol. Toxicol. 13, 47–52.

Tomizawa, K., Sugano, K., Yamada, H., Horii, I., 2006. Physicochemical and cell-based approach for early screening of phospholipidosis-inducing potential. J. Toxicol. Sci. 31, 315–324.

Urushidani, T., Nagao, T., 2005. Toxicogenomics: the Japanese initiative. In: Borlak, J. (Ed.), Handbook of Toxicogenomics—Strategies and Applications. Wiley-VCH, pp. 623–631.

Weber, L.W., Boll, M., Stampfl, A., 2003. Hepatotoxicity and mechanism of action of haloalkanes: carbon tetrachloride as a toxicological model. Crit. Rev. Toxicol. 33, 105–136.

Whitehouse, L.W., Menzies, A., Mueller, R., Pontefract, R., 1994. Ketoconazole-induced hepatic phospholipidosis in the mouse and its association with de-*N*-acetyl ketoconazole. Toxicology 94, 81–95.

Xia, Z., Ying, G., Hansson, A.L., Karlsson, H., Xie, Y., Bergstrand, A., DePierre, J.W., Nassberger, L., 2000. Antidepressant-induced lipidosis with special reference to tricyclic compounds. Prog. Neurobiol. 60, 501–512.

Please cite this article as: Hirode, M., et al., Gene expression profiling in rat liver treated with compounds inducing phospholipidosis, Toxicol. Appl. Pharmacol. (2008), doi:10.1016/j.taap.2008.01.036

Human & Experimental Toxicology (2008) xxx: 1–13
www.het.sagepub.com

Species-specific differences in coumarin-induced hepatotoxicity as an example toxicogenomics-based approach to assessing risk of toxicity to humans

T Uehara[1], N Kiyosawa[1], T Shimizu[1], K Omura[1], M Hirode[1], T Imazawa[1], Y Mizukawa[2], A Ono[1], T Miyagishima[1], T Nagao[3] and T Urushidani[1,2]

[1]Toxicogenomics Project, National Institute of Biomedical Innovation, Ibaraki, Osaka, Japan; [2]Department of Pathophysiology, Faculty of Pharmaceutical Sciences, Doshisha Women's College of Liberal Arts, Kyotanabe, Kyoto, Japan; and [3]National Institute of Health Sciences, Setagaya-ku, Tokyo, Japan

One expected result from toxicogenomics technology is to overcome the barrier because of species-specific differences in prediction of clinical toxicity using animals. The present study serves as a model case to test if the well-known species-specific difference in the toxicity of coumarin could be elucidated using comprehensive gene expression data from rat in-vivo, rat in-vitro, and human in-vitro systems. Coumarin 150 mg/kg produced obvious pathological changes in the liver of rats after repeated administration for 7 days or more. Moreover, 24 h after a single dose, we observed minor and transient morphological changes, suggesting that some early events leading to hepatic injury occur soon after coumarin is administered to rats. Comprehensive gene expression changes were analyzed using an Affymetrix GeneChip® approach, and differentially expressed probe sets were statistically extracted. The changes in expression of the selected probe sets were further examined in primary cultured rat hepatocytes exposed to coumarin, and differentially expressed probe sets common to the in-vivo and in-vitro datasets were selected for further study. These contained many genes related to glutathione metabolism and the oxidative stress response. To incorporate human data, human hepatocyte cultured cells were exposed to coumarin and changes in expression of the bridging gene set were examined. In total, we identified 14 up-regulated and 11 down-regulated probe sets representing rat–human bridging genes. The overall responsiveness of these genes to coumarin was much higher in rats than humans, consistent with the reported species difference in coumarin toxicity. Next, we examined changes in expression of the rat–human bridging genes in cultured rat and human hepatocytes treated with another hepatotoxicant, diclofenac sodium, for which hepatotoxicity does not differ between the species. Both rat and human hepatocytes responded to the marker genes to the same extent when the same concentrations of diclofenac sodium were exposed. We conclude that toxicogenomics-based approaches show promise for overcoming species-specific differences that create a bottleneck in analysis of the toxicity of potential therapeutic treatments.

Q1

Key words: coumarin; hepatocyte; hepatotoxicity; human; liver; rat; toxicogenomics

Introduction

The Toxicogenomics Project (TGP) is a 5-year collaborative project of the National Institute of Health Sciences, the National Institute of Biomedical Innovation, and 15 pharmaceutical companies in Japan that began in 2002.[1] The aim was to construct a large-scale toxicology database of transcriptomes useful to predict the toxicity of new chemical entities in early stages of drug development. About 150 chemicals, primarily medicinal compounds, were selected and gene expression in the rat liver (also kidney in some cases) or rat and human hepatocytes was comprehensively analyzed by using the Affymetrix GeneChip®.[2] In 2007, the project was completed and the whole system, consisting of a database, an analysis system, and a prediction system, was completed and named TG-GATEs (for Genomics Assisted Toxicity Evaluation System developed by Toxicogenomics Project in Japan).

Correspondence to: Tetsuro Urushidani, Department of Pathophysiology, Faculty of Pharmaceutical Sciences, Doshisha Women's College of Liberal Arts, Kodo, Kyotanabe, Kyoto 610-0395, Japan. Email: turushid@dwc.doshisha.ac.jp

10.1177/0960327107087910

The main purpose of creating the system was to facilitate analysis of the mechanisms of toxicity and prediction of chronic toxicity from acute data in preclinical studies, and the consensus response to the project is that toxicogenomics-based technologies provide a useful tool. However, the final goal of a preclinical study should be prediction of clinical toxicity based on animal data. Toward this end, overcoming species-specific differences has proved to be the most difficult problem. We expect that elucidation of mechanisms of toxicity using toxicogenomics-based tools should lead to an improved ability to use animal data to make reasonable predictions of toxicity in humans.[3] However, there have been few reports of species-specific differences in the toxicological response at the level of changes in gene expression.[4]

We obtained gene expression data from rat primary hepatocytes as well as human frozen hepatocytes (in addition to rat in-vivo liver) to build an informational bridge between the two species. In the present study, we analyzed the effects of coumarin, a representative hepatotoxicant with a known species-specific difference in toxicity, as a model case for determining if species-specific differences in hepatotoxicity can be accurately predicted using a toxicogenomics-based approach.

Materials and methods

Chemicals

Coumarin and diclofenac sodium (DFNa) were obtained from Tokyo Chemical Industry (Tokyo, Japan).

Animal Treatment

All experimental protocols using animals were reviewed and approved by the Ethics Review Committee for Animal Experimentation of the National Institute of Health Sciences. The experimental protocols using human hepatocytes were reviewed and approved by both the Ethics Review Committees for Experimentation on Human Subjects of the National Institute of Health Sciences and of the National Institute of Biomedical Innovation.

Five-week-old male Sprague-Dawley rats were obtained from Charles River Japan Inc. (Kanagawa, Japan). After a 7-day quarantine and acclimatization period, 6-week-old animals were assigned to dosage groups (five rats per group) using a computerized stratified random grouping method based on individual body weight. The animals were individually housed in stainless-steel cages in an animal room that was lighted for 12 h (7:00–19:00) daily, ventilated with an air-exchange rate of 15 times per hour and maintained at 21–25 °C with a relative humidity of 40–70%. Each animal was allowed free access to water and pellet diet (CRF-1, sterilized by radiation; Oriental Yeast Co., Ltd., Tokyo, Japan).

Either vehicle (corn oil), or 15, 50, or 150-mg/kg coumarin was administered orally to rats once daily on day 1, 3, 7, 14, and 28, and the animals were euthanized 24 h after the last dosing by exsanguination from the abdominal aorta under ether anesthesia. Liver samples were obtained from the left lateral lobe of the liver of each animal immediately after sacrifice. For light microscopy, liver samples were fixed in 10% neutral-buffered formalin, dehydrated in alcohol, and embedded in paraffin. Paraffin sections were prepared and stained using standard methods for hematoxylin and eosin staining. Histopathological findings were graded into four categories: very slight, slight, moderate, and severe. For electron microscopy, a piece of tissue from the liver was fixed in 2.5% glutaraldehyde solution. Ultra-thin sections, stained with Mayer's hematoxylin and lead citrate after standard tissue processing, were observed under a Hitachi electron microscope (H-7650; Tokyo, Japan). Q2

Hepatocyte treatment

Hepatocytes were isolated from 6-week-old male Sprague-Dawley rats under sodium pentobarbital (120 mg/kg, i.p.) and anesthetized using a modified two-step collagenase perfusion method. The liver was perfused via the portal vein for 10 min with divalent, cation-free, EGTA (0.5 mM)-supplemented Q3 HEPES-buffered Hank's balanced salt solution fol- Q4 lowed by a 10-min perfusion with HEPES (10 mM)-buffered normal Hank's balanced salt solution containing soybean trypsin inhibitor (0.05 g/L, T-2011; Sigma Aldrich, St Louis, Missouri, USA) and collagenase (0.5 g/L, 034-10533; Wako Pure Chemical Industries, Osaka, Japan) at a flow rate of 10–30 mL/min. The isolated cells were washed three times and centrifugated at 50 × *g* for 1 min to obtain a parenchymal cell-enriched pellet. Hepatocytes were not used when their viability was <70% (as assessed by trypan blue exclusion). Cell samples that passed the threshold for viability were seeded into collagen-coated six-well plates (BD BioCoat™ Collagen I Cellware; BD Bioscience, Bedford, Massachusetts, USA) at a density of 1×10^6 cells/well in 2 mL HMC Bulletkit medium (Cambrex, Walkersville, Maryland, USA) supplemented with 10% fetal bovine serum.

For human hepatocytes (Tissue Transformation Technologies Inc., presently BD Biosciences, San Jose, California, USA), the frozen cells were thawed, washed twice with medium (L15 medium supplemented with penicillin, streptomycin, and 10% fetal bovine serum), and then seeded as described for rat hepatocytes except that the cell density was 1.2×10^6 cells/well.

Following an attachment period of 3 h, the medium was replaced and kept overnight before exposure to the drug at 37 °C in an atmosphere of 5% CO_2. The test compounds were added to the medium directly or as a 1000× stock solution in dimethylsulfoxide (DMSO). After 2, 8, or 24-h exposure, cells were dissolved with RLT buffer (Qiagen, Valencia, California, USA) and collected for expression profiling. GeneChip analysis was performed in duplicate for each concentration.

Cell viability was assessed by monitoring leakage of lactate dehydrogenase (LDH). To do this, both the culture medium and the cell lysate (lysis with 0.1% Triton X-100) were analyzed using an automatic biochemical analyzer (TBA-200FR; Toshiba, Tokyo, Japan) and the rate of survival relative to a control was calculated as follows: $LDH_{cell}/(LDH_{cell} + LDH_{medium})$.

The appropriate concentrations of test drugs were determined in a preliminary experiment. For our general protocol, the highest concentration was set to 10–20% of the lethal concentration as estimated by LDH leakage over 24 h. When the cells could tolerate as much as 10 mM or the level equal to the solubility limit of the compound in DMSO (allowed to add up to 0.1% in the final concentration), the highest concentration was set to either value. Exposures were performed at two different concentrations, 1/5 and 1/25 of the highest concentration. In case of coumarin, no LDH leakage was observed for either rat or human hepatocytes after treatment with concentrations of up to 300 μM, which was the solubility limit. Thus, concentrations of 12, 60, and 300 μM coumarin were used in subsequent assays. For DFNa, 400 μM was set as the maximum both in rats and humans. Thus, concentrations of 16, 80, and 400 μM DFNa were used in subsequent assays.

GeneChip analysis

For analysis of rat livers, microarray analysis was conducted on three of five samples from each single dose group (24-h post-dose) using GeneChip® RAE 230A probe arrays (Affymetrix, Santa Clara, California, USA). Liver samples were homogenized with buffer RLT supplied with the RNeasy Mini Kit (Qiagen) and total RNA was isolated according to the manufacturer's instructions.

For hepatocytes, GeneChip analysis was performed in duplicate for each concentration using RAE230 2.0 probe arrays for rat hepatocytes and U133 Plus 2.0 arrays for human hepatocytes (Affymetrix). Cells were dissolved with RLT buffer and collected for expression profiling. Different versions were used for the in-vitro versus the in-vivo study because RAE230 2.0 was released after the in-vivo experiments were completed. The procedure was conducted basically as described in the manufacturer's instructions using Superscript Choice System (Invitrogen, Carlsbad, California, USA) and T7-(dT)24-oligonucleotide primer (Affymetrix) for cDNA synthesis, cDNA Cleanup Module (Affymetrix) for purification, and BioArray High yield RNA Transcript Labeling Kit (Enzo Diagnostics, Farmingdale, New York, USA) for synthesis of biotin-labeled cRNA. Ten micrograms of fragmented cRNA was hybridized to a RAE230A probe array for 18 h at 45 °C at 60 rpm, after which the array was washed and stained with streptavidin–phycoerythrin using Fluidics Station 400 (Affymetrix) and scanned with a Gene Array Scanner (Affymetrix). The digital image files were processed using Affymetrix Microarray Suite version 5.0. Microarray image data were analyzed with GeneChip Operating Software (Affymetrix). All microarray data were scaled by global normalization with the mean signal intensity of all data adjusted to 500.

Gene expression data analysis

To identify genes that are differentially expressed after in-vivo coumarin treatment, the Student's *t*-test was applied with a *P* value cut-off of 0.05 in combination with fold changes of 2.0 or greater and 0.5 or less using Spotfire® DecisionSite for Functional Genomics (Spotfire, Göteborg, Sweden). Probe sets designated as absent by an Affymetrix detection call in any of six samples (three each for control and treated) were excluded from further analysis.

To extract genes that changed in response to coumarin in both the in-vivo and in-vitro sample groups, the changes in expression of the above-mentioned probe sets were examined in rat hepatocytes treated with the high dose (300 μM) of coumarin. Probe sets showing 1.5-fold or greater (up-regulated) and 0.6-fold or less (down-regulated) were selected.

In the next step, the genes in common to the in-vivo and in-vitro rat assays were compared in rat versus human hepatocytes. To do this, we first examined public data on human orthologs of the rat genes (NetAffx[5]). Upon assignment of orthologs,

rat probes sets without human ortholog information were excluded. Because for the redundant probe sets for human samples, a single probe set was selected based on the reliability and dose-dependency of the expression profile. Finally, the probe sets, which were designated as absent by Affymetrix detection, call in seven or more out of eight samples (two each for control and high dose treated in rat and human) were excluded from further analysis.

To facilitate analysis in the large-scale microarray database, we developed two types of one-dimensional score, TGP1 and TGP2, which express the trends in changes in expression of biomarker genes as a whole. The former is based on the signal log ratio[6] and is convenient for comparing the responsiveness of several drugs to a marker gene list. The disadvantages of this scoring system are that it overestimates responsiveness when the list contains a gene for which induction is extreme (such as CYP1A1) and it underestimates responsiveness when genes in the list are mobilized in either direction. To overcome these disadvantages, we used another score, TGP2, which is based on the size of the effects $g = l\mu_2 - \mu_1 l/\sigma_{pooled}$, where

$$\sigma_{pooled} = \sqrt{\frac{(N_1-1)\sigma_1 + (N_2-1)\sigma_2{}^2}{(N_1+N_2-2)}}$$

To obtain an unbiased estimate of the effect size d = c × d, where c is bias correction[7]

$$c = 1-\frac{3}{4(N_1+N_2-2)-1}$$

The corrected effect size was calculated for each probe set in the marker gene list, summed, and divided by the number of probe sets in the list, and finally multiplied by 100 to obtain the TGP2 score used in the present study.

Results

Changes in rat livers in response to treatment with coumarin

We noted several pathological changes in rat livers after administration of coumarin (Table 1). Twenty-four hour after a single dose of coumarin, no abnormal morphological changes were observed by light microcopy (Figure 1a,b). However, histopathological changes became apparent with repeated administration of coumarin for 1 week or later in the highest dose group, and degenerative lesions, such as vacuolar degeneration and intracytoplasmic inclusion bodies, were evident at day 29 post-initiation of treatment (Figure 1c,d). From day 4 to day 29, single cell necrosis of hepatocytes was occasionally observed.

We next used electron microscopy to look for subtle changes that may be apparent 24 h after a single dose of coumarin. The analysis showed dilation of

Table 1 Histopathological findings in rat livers treated with coumarin

Histopathological findings	*Time Point (days)*	*2*			*4*			*8*			*15*			*29*		
	Dose (mg/kg)	*15*	*50*	*150*	*15*	*50*	*150*	*15*	*50*	*150*	*15*	*50*	*150*	*15*	*50*	*150*
	Number of animals examined	*5*	*5*	*5*	*5*	*5*	*5*	*5*	*5*	*5*	*5*	*5*	*5*	*5*	*5*	*5*
Hepatocyte / Single cell necrosis		0	0	0	0	0	1	0	0	1	0	0	1	0	0	2
very slight							1			1			1			2
Hepatocyte / Inclusion body, intracytoplasmic		0	0	0	0	0	0	0	0	5	0	0	5	0	0	5
very slight										5			2			
slight													3			2
moderate																3
Hepatocyte, centrilobular / Hypertrophy		0	0	0	0	0	0	0	0	3	0	0	5	0	0	5
very slight										3			2			1
slight													3			4
Hepatocyte, centrilobular / Degeneration, vacuolar		0	0	0	0	0	0	0	0	0	0	0	3	0	0	5
very slight													2			
slight													1			5

Vehicle alone or coumarin 15, 50, or 150 mg/kg was administered orally to rats once daily for 1, 3, 7, 14, and 28 days, and the animals were euthanized 24 h after the last dosing, namely, on 2, 4, 8, 15, and 29 days ($n = 5$). The pathological change in the liver was graded into four categories: very slight, slight, moderate, and severe. The number of animals having the morphology at each grade is shown.

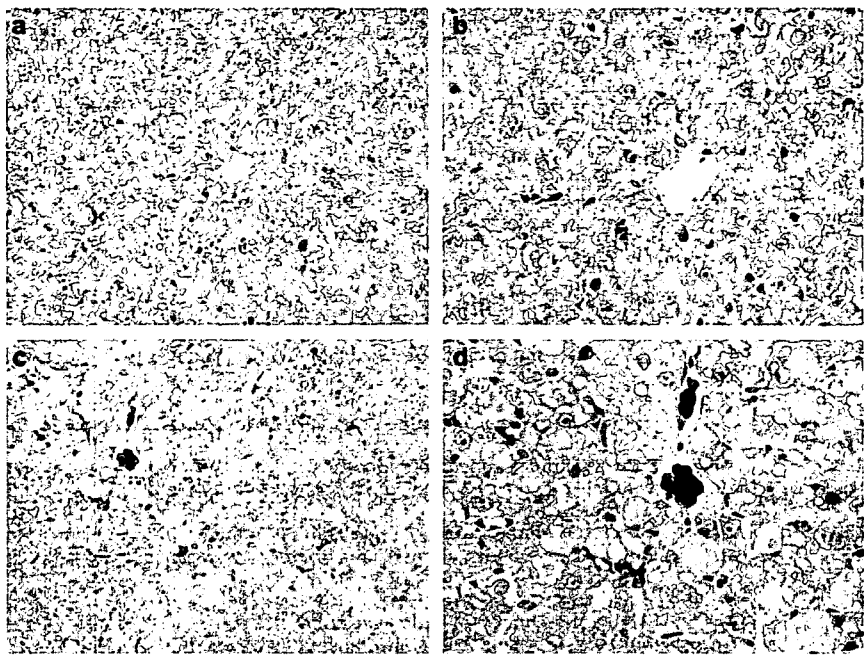

Figure 1 Histopathological changes in the rat liver treated with 150 mg/kg coumarin. (a) Low (×100) and (b) high (×200) magnification micrographs of a liver treated once with 150 mg/kg coumarin (24 h after a single dose). No abnormal morphological changes were detected in the control liver. (c) Low (×100) and (d) high (×200) magnification images of a liver treated with 150 mg/kg coumarin once a day for 28 days. Degenerative changes, such as vacuolation of hepatocytes, are evident after repeated administration of coumarin.

the rough endoplasmic reticulum of hepatocytes in the centrilobular region of the liver in the highest dose group (Figure 2). This early slight ultrastructural change was considered to be consistent with hepatic injury we observed after repeated exposure to the drug. Thus, the 24-h post-treatment time point seemed appropriate for microarray analysis, as at the cellular level, coumarin had already begun exerting an effect at 24-h post-single treatment.

As described in the Methods section, statistically significant up- (136 probe sets) and down-regulated genes (79 probe sets) were extracted and these are listed in Tables 2 and 3. In livers treated with coumarin, the following genes were remarkably mobilized, that is, genes involved in glutathione metabolism and oxidative stress: "glutathione reductase", "glutathione-S-transferase, pi 1/2", "glutathione S-transferase Yc2 subunit", "microsomal glutathione S-transferase 2", "glutamate-cysteine ligase, catalytic

Q6

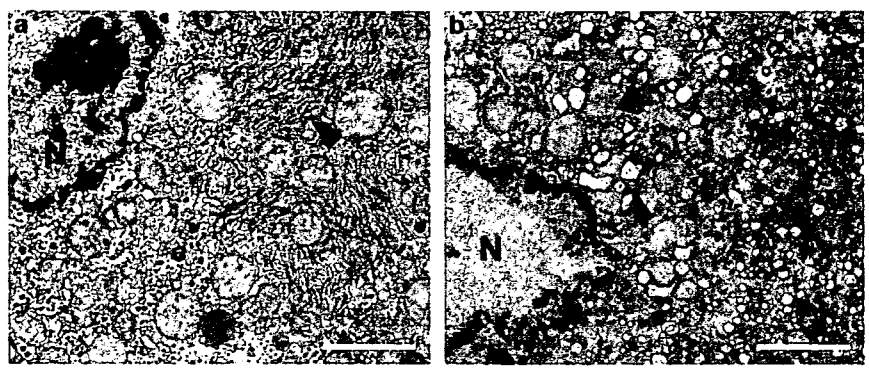

Figure 2 Early detection of coumarin-induced changes by electron microscopy. (a) Control hepatocyte, (b) coumarin-treated hepatocyte (150 mg/kg; 24 h after a single dose). Expansion of the rough endoplasmic reticulum (rER) in the coumarin-treated hepatocyte as compared with a control is evident. N, nucleus; Arrowhead, rER; Bar = 2 μm.

Table 2 Genes up-regulated in the rat liver 24 h after administration of coumarin

Affymetrix probe set ID	*Gene symbol*	*Gene description*	*Fold change*		
			Dose (mg/kg)		
			15	*50*	*150*
1371817_at	LOC290651	Similar to myo-inositol 1-phosphate synthase A1	9.52		26.50
1388122_at	Gstp1/Gstp2	Glutathione-S-transferase, pi 1/pi 2	2.84	1.57	13.00
1369698_at	Abcc3	ATP-binding cassette, sub-family C (CFTR/MRP), member 3	4.41	2.59	11.58
1370342_at	Kcnk2	Potassium channel, subfamily K, member 2	2.45	3.22	10.87
1368013_at	Ddit4l	DNA-damage-inducible transcript 4-like	1.71	1.41	9.07
1388271_at	LOC682651/LOC689415	Similar to Metallothionein-2 (MT-2) (Metallothionein-II) (MT-II)	1.39	1.40	8.81
1375213_at	Pck2_predicted	Phosphoenolpyruvate carboxykinase 2 (mitochondrial) (predicted)	3.07	1.97	6.09
1371237_a_at	Mt1a	Metallothionein 1a	1.52	1.70	5.92
1368121_at	Akr7a3	Aldo-keto reductase family 7, member A3 (aflatoxin aldehyde reductase)	3.43	2.00	5.78
1387599_a_at	Nqo1	NAD(P)H dehydrogenase, quinone 1	2.68	2.33	5.77
1371970_at	RGD1560913_predicted	Similar to expressed sequence AW413625 (predicted)	2.92	1.19	5.67
1371089_at	—	Transcribed locus	2.25	1.38	5.29
1379740_at	LOC361346	Similar to chromosome 18 open reading frame 54	2.29	2.32	4.96
1387693_a_at	Slc6a9	Solute carrier family 6 (neurotransmitter transporter, glycine), member 9	1.66	0.97	4.94
1372510_at	Srxn1	Sulfiredoxin 1 homolog	1.19	0.95	4.91
1370902_at	Akr1b8	Aldo-keto reductase family 1, member B8	2.20	1.96	4.69
1369772_at	Slc6a9	Solute carrier family 6 (neurotransmitter transporter, glycine), member 9	1.45	0.92	4.42
1368247_at	Hspa1a /Hspa1b	Heat shock 70kD protein 1A/1B (mapped)	2.18	1.94	4.22
1387925_at	Asns	Asparagine synthetase	1.40	1.35	4.06
1376051_at	Cryl1	Crystallin, lamda 1	1.25	1.24	3.94
1367847_at	Nupr1	Nuclear protein 1	1.24	1.46	3.86
1368143_at	Anxa7	Annexin A7	1.68	1.38	3.77
1377016_at	Creld2	Cysteine-rich with EGF-like domains 2	0.88	0.94	3.75
1373043_at	LOC680945/LOC683036	Similar to stromal cell–derived factor 2-like 1	1.86	1.99	3.71
1388102_at	Ltb4dh	Leukotriene B4 12-hydroxydehydrogenase	1.44	1.05	3.59
1372653_at	Fkbp11	FK506 binding protein 11	1.64	1.42	3.54
1373810_at	Pla2g12a_predicted	Phospholipase A2, group XIIA (predicted)	1.42	1.96	3.53
1376247_at	—	Transcribed locus	1.97	1.39	3.52
1371442_at	Hyou1	Hypoxia up-regulated 1	1.26	0.88	3.50
1372985_at	Zfp444_predicted	Zinc finger protein 444 (predicted)	2.10	1.28	3.47
1373787_at	Slc6a9	Solute carrier family 6 (neurotransmitter transporter, glycine), member 9	1.35	1.02	3.30
1394080_at	—	Transcribed locus	2.66	2.54	3.17
1373850_at	Smpdl3b	Sphingomyelin phosphodiesterase, acid-like 3B	1.46	1.23	3.07
1370073_at	Dnajc3	Protein kinase inhibitor p58	1.53	1.31	3.06
1374036_at	Mcm2_predicted	Minichromosome maintenance deficient 2 mitotin (predicted)	1.55	0.85	3.06
1370912_at	Hspa1b	Heat shock 70kD protein 1B (mapped)	1.64	1.46	3.01
1377145_at	LOC362068	Similar to monogenic, audiogenic seizure susceptibility 1	1.56	1.63	2.99
1392920_at	Ell3	Elongation factor RNA polymerase II-like 3	1.62	1.41	2.96
1376668_at	RGD1311126_predicted	Similar to RIKEN cDNA 4922503N01 (predicted)	0.92	0.79	2.94
1389308_at	Dnajb11	DnaJ (Hsp40) homolog, subfamily B, member 11	1.42	1.14	2.91
1376055_at	Mcm5_predicted	Minichromosome maintenance deficient 5, cell division cycle 46 (predicted)	1.81	1.07	2.90
1375852_at	Hmgcr	3-hydroxy-3-methylglutaryl-Coenzyme A reductase	1.28	0.91	2.90
1386958_at	Txnrd1	Thioredoxin reductase 1	1.07	0.81	2.89
1371210_s_at	RT1-Aw2	RT1 class Ib, locus Aw2	1.50	1.72	2.88
1372390_at	—	Transcribed locus	1.25	0.81	2.86
1374359_at	Ccne2_predicted	Cyclin E2 (predicted)	1.24	0.91	2.85
1370665_at	Hyou1	Hypoxia up-regulated 1	1.03	0.87	2.84
1387212_at	Bhlhb8	Basic helix-loop-helix domain containing, class B, 8	1.51	2.29	2.81
1374805_at	RGD1561749_predicted	Similar to hypothetical protein MGC5528 (predicted)	2.25	1.13	2.81
1389578_at	Isrip	Ischemia/reperfusion inducible protein	1.23	1.25	2.73
1370429_at	RT1-Aw2	RT1 class Ib, locus Aw2	1.89	1.29	2.70
1370803_at	Zwint	ZW10 interactor	1.58	1.23	2.68
1370688_at	Gclc	Glutamate-cysteine ligase, catalytic subunit	1.06	0.64	2.67
1377037_at	LOC679253/LOC681337	Similar to Acyl-coA thioesterase 4	1.32	0.96	2.65
1375428_at	Creg_predicted	Cellular repressor of E1A-stimulated genes (predicted)	1.24	1.17	2.65
1374048_at	Nrtn	Neurturin	1.61	1.63	2.64
1377334_at	RT1-Ba	RT1 class II, locus Ba	1.86	1.85	2.63

(continued)

Table 2 *(continued)*

Affymetrix probe set ID	*Gene symbol*	*Gene description*	*Fold change*		
			Dose (mg/kg)		
			15	*50*	*150*
1388628_at	Tmed3	Transmembrane emp24 domain containing 3	1.40	1.17	2.59
1367733_at	Ca2	Carbonic anhydrase 2	1.11	0.86	2.59
1373557_at	Mcm4	Minichromosome maintenance deficient 4 homolog	1.51	0.90	2.57
1368544_a_at	Nol3	Nucleolar protein 3	1.30	1.67	2.57
1372954_at	—	Sprague-Dawley UV73 mRNA, partial sequence	1.37	1.80	2.54
1369061_at	Gsr	Glutathione reductase	1.27	1.09	2.53
1370007_at	Pdia4	Protein disulfide isomerase associated 4	1.10	0.98	2.53
1389391_at	RGD1564876_predicted	Similar to solute carrier family 35, member E3 (predicted)	1.26	0.98	2.50
1372523_at	Gclc	Glutamate-cysteine ligase, catalytic subunit	1.17	0.79	2.50
1390591_at	Slc17a3	Na/Pi cotransporter 4	1.67	1.07	2.49
1368376_at	Nr0b2	Nuclear receptor subfamily 0, group B, member 2	1.74	1.69	2.49
1398791_at	Txnrd1	Thioredoxin reductase 1	1.10	0.89	2.48
1367938_at	Ugdh	UDP-glucose dehydrogenase	1.28	0.96	2.46
1387022_at	Aldh1a1	Aldehyde dehydrogenase family 1, member A1	2.15	1.21	2.44
1373613_at	LOC300191	Similar to RIKEN cDNA 4930570C03	1.09	0.96	2.44
1372406_at	Mcm3_predicted	Minichromosome maintenance deficient 3 (predicted)	1.65	0.81	2.43
1374121_at	—	Transcribed locus	2.32	1.82	2.41
1372261_at	—	Transcribed locus	1.23	1.13	2.41
1384130_at	RGD1560171_predicted	Similar to PRO0149 protein (predicted)	1.63	2.13	2.39
1380030_at	Znf593_predicted	Zinc finger protein 593 (predicted)	1.09	0.88	2.38
1389671_at	Trpc2	Transient receptor potential cation channel, subfamily C, member 2	1.21	1.29	2.36
1373445_at	Nol8_predicted	Nucleolar protein 8 (predicted)	1.24	0.85	2.36
1387083_at	Ctf1	Cardiotrophin 1	1.18	0.96	2.35
1377135_at	Alox5	Arachidonate 5-lipoxygenase	1.00	1.25	2.34
1375088_at	—	Transcribed locus	0.98	1.14	2.31
1369588_a_at	Atpif1	ATPase inhibitory factor 1	1.27	1.13	2.30
1398341_at	RGD1559720_predicted	RGD1559720 (predicted)	1.03	1.09	2.29
1389767_at	RGD1304924_predicted	Similar to hypothetical protein FLJ31364 (predicted)	1.13	1.18	2.29
1374249_at	RGD1304580	Similar to Hypothetical protein MGC38513	0.93	1.10	2.28
1373530_at	Ccne1	cyclin E	1.06	0.52	2.28
1371113_a_at	Tfrc	Transferrin receptor	1.28	0.76	2.28
1370127_at	Pold1	Polymerase (DNA directed), delta 1, catalytic subunit	1.42	1.37	2.28
1376073_at	Sel1h	Sel1 (suppressor of lin-12) 1 homolog	1.40	1.06	2.26
1392841_at	—	Transcribed locus	1.39	2.02	2.23
1398879_at	Tmem66	Transmembrane protein 66	1.25	1.07	2.22
1388622_at	Nol5a	Nucleolar protein 5A	1.46	1.19	2.22
1371583_at	Rbm3	RNA binding motif protein 3	1.19	1.16	2.21
1387188_at	Slc17a1	Solute carrier family 17, member 1	1.37	1.33	2.20
1368037_at	Cbr1	Carbonyl reductase 1	0.96	1.01	2.20
1390430_at	Nr1d2	Nuclear receptor subfamily 1, group D, member 2	0.97	1.05	2.19
1398788_at	Pdia3	Protein disulfide isomerase associated 3	1.43	1.24	2.19
1386922_at	Ca2	Carbonic anhydrase 2	1.07	0.83	2.19
1367983_at	Fen1	Flap structure–specific endonuclease 1	1.59	1.12	2.16
1373999_at	—	Transcribed locus	1.27	0.83	2.16
1376781_at	Glb1_mapped	Galactosidase, beta 1 (mapped)	1.20	1.03	2.14
1381968_at	Sema6d_predicted	Sema domain, transmembrane domain (TM), and cytoplasmic domain, (semaphorin) 6D (predicted)	1.18	1.20	2.13
1372774_at	Coq6	Coenzyme Q6 homolog	1.30	0.90	2.13
1376098_a_at	Lad1_predicted	Ladinin (predicted)	1.02	1.03	2.12
1370904_at	Hla-dma	Major histocompatibility complex, class II, DM alpha	1.32	1.11	2.12
1389805_at	—	—	1.27	1.29	2.11
1388331_at	Tra1_predicted	Tumor rejection antigen gp96 (predicted)	1.08	0.93	2.11
1386466_at	—	Transcribed locus	1.08	1.24	2.11
1372599_at	Mgst2_predicted	Microsomal glutathione S-transferase 2 (predicted)	1.34	1.34	2.11
1372471_at	—	Transcribed locus	1.66	1.03	2.10
1372247_at	Ddost_predicted	Dolichyl-di-phosphooligosaccharide-protein glycotransferase (predicted)	1.26	1.15	2.10
1370055_at	Rab3d	RAB3D, member RAS oncogene family	0.72	0.77	2.10
1398596_at	—	Transcribed locus	2.07	1.65	2.09
1387783_a_at	Acaa1	Acetyl-coenzyme A acyltransferase 1	1.49	1.20	2.09
1373908_at	—	—	1.71	1.40	2.09
1398383_at	Cyb561_predicted	Cytochrome b-561 (predicted)	1.40	1.15	2.07
1377350_at	—	Transcribed locus	1.74	1.26	2.07
1370428_x_at	RT1-Aw2	RT1 class Ib, locus Aw2	1.66	1.50	2.07

(continued)